Universidade de Coimbra
Faculdade de Ciências e Tecnologia

Small-scale photovoltaic systems: investigation of energy harvesting applications and development of a phone charging system

David de Sousa Nunes Teixeira

Thesis submitted for the degree of Master of Science
in Physics Engineering

July 2014

Universidade de Coimbra
Faculdade de Ciências e Tecnologia

Small-scale photovoltaic systems: investigation of energy harvesting applications and development of a phone charging system

David de Sousa Nunes Teixeira

Thesis submitted for the degree of Master of Science
in Physics Engineering

Under the supervision of:
Dr. Manuela Silva
Dr. Jurjen Winkel

July 2014

Abstract

This thesis concerns the development of a system for the measurement of organic photovoltaic module characteristics, as well as a low-cost application product for mobile phone charging. All work was realised during an internship at a company which produces and commercialises organic photovoltaic devices, head-quartered in Cambridge, UK – Eight19.

The measurement system is focused on enabling the assessment of photovoltaic module performance in low-light situations, with the possibility of being used for energy harvesting. This system is based on a microcontroller which, through an electronic circuit for interfacing with the module, measures its short-circuit current and the open-circuit voltage, allowing for a posterior calculation of its maximum power. Some results of this system are presented under different lighting conditions.

Regarding the phone charging application, a study is firstly presented, concerning the availability of solar energy in Africa, which corresponds to the target market of the company where this work was done. Following this, some prototypes for this application are planned and developed, based on different options for energy use and storage, allowing for comparison.

Keywords: photovoltaic modules; low-cost application; phone charging; energy harvesting

Resumo

Esta tese aborda o desenvolvimento de um sistema de medida de características de módulos fotovoltaicos orgânicos, bem como uma aplicação de baixo custo destes módulos, para o carregamento de telemóveis. Todo o trabalho foi realizado em estágio, numa empresa que produz e comercializa módulos fotovoltaicos orgânicos, sediada em Cambridge, no Reino Unido – Eight19.

O sistema de medida tem o intuito de permitir uma avaliação do desempenho dos módulos fotovoltaicos em situações de fraca iluminação, com a possibilidade de serem utilizados para *energy harvesting*. Este sistema baseia-se num micro-controlador que, através de um circuito electrónico de interface com o módulo fotovoltaico, mede a corrente de curto-circuito e a tensão em circuito aberto do mesmo, permitindo um cálculo posterior da sua potência máxima. São apresentados alguns resultados deste sistema em diferentes condições de iluminação.

Quanto à aplicação de carregamento de telemóveis, é primeiro efectuado um estudo acerca da energia solar disponível em África, que corresponde ao mercado-alvo da empresa onde este trabalho foi realizado. De seguida são planeados e desenvolvidos protótipos para esta aplicação, baseados em diferentes hipóteses de aproveitamento de energia, permitindo a sua comparação.

Palavras-chave: módulos fotovoltaicos; aplicação de baixo custo; carregamento de dispositivos móveis; *energy harvesting*

Acknowledgements

I would like to express my gratitude to Dr. Michael Niggemann and Dr. Christoph Sele, both of whom provided their experience, knowledge and patience over the course of the internship to ensure I would be able to develop a thorough and relevant work. Their assistance always steered me in the right direction and helped me stay focused on what is important. I thank them for all the support, which helped not only with this work, but also with my future professional life.

To everyone at Eight19, thank you for a wonderful experience, which definitely helped me grow as an individual and left me much better prepared for the workplace. Every single one at the company has taught me a lot about myself and I will always remember these 6 months.

I would like to thank Professor Manuela Silva for the preoccupation, availability and support demonstrated throughout my entire academic life, in particular during the duration of this internship. Thank you for the advice and suggestions which were undoubtedly important for my growth as a professional.

To all my colleagues and friends which, one way or another, have been a part of my life and with whom I have shared and hope to continue to share great moments. A special thanks to Xénon for the friendship through these 11 years, for the adventures and good times.

A huge thank you to my parents, brothers and aunt, for being with me since the beginning and always, no matter what life may bring. For providing me with this amazing opportunity. In particular, a thank you to my parents, who brought me into the world, raised me and continue to make me grow.

Finally, and so importantly, I would like to thank Patrícia for all the dimensions she brought into my life, for the unconditional support, for saying the right words and for making me a better person. Thank you.

Agradecimentos

Gostaria de expressar a minha gratidão ao Dr. Michael Niggemann e Dr. Christoph Sele, que contribuíram com a sua experiência, sabedoria e paciência ao longo deste estágio, para garantir que o trabalho por mim desenvolvido seria completo e relevante. O seu auxílio guiou-me sempre na direcção certa e ajudou-me a concentrar no que é importante. Obrigado por todo o apoio, que me ajudou não só com este trabalho, mas também com a minha futura vida profissional.

A toda a gente na Eight19, obrigado pela experiência maravilhosa, que me ajudou sem dúvida a crescer como indivíduo e deixou-me melhor preparado para trabalhar. Cada pessoa na empresa ensinou-me muito acerca de mim mesmo e irei sempre recordar estes 6 meses.

Gostaria de agradecer à Professora Manuela Silva pelo acompanhamento, disponibilidade e apoio demonstrados durante todo o meu percurso lectivo e em especial durante a duração deste estágio. Obrigado pelos conselhos e sugestões que sem dúvida foram uma mais-valia para o meu crescimento como profissional.

A todos os meus colegas e amigos que, de uma forma ou de outra, têm participado na minha vida e com quem partilhei e espero continuar a partilhar óptimos momentos. Um agradecimento especial ao Xénon pela amizade ao longo destes 11 anos, pelas aventuras e bons momentos.

Um enorme obrigado aos meus pais, irmãos e tia, por me acompanharem desde sempre e por estarem sempre presentes, independentemente do que a vida possa trazer. Por me terem dado esta grande oportunidade e terem tornado tudo possível. Em especial, obrigado aos meus pais, que me trouxeram ao Mundo, me educaram e continuam a fazer-me crescer.

Por fim, e tão importante, um agradecimento à Patrícia por todas as dimensões que trouxe à minha vida, pelo apoio incondicional, pelas palavras certas e por fazer de mim uma pessoa melhor. Obrigado.

I do not think there is any thrill that can go through the human heart like that felt by the inventor as he sees some creation of the brain unfolding to success... Such emotions make a man forget food, sleep, friends, love, everything.

– Nikola Tesla

Contents

List of Figures

List of Tables

List of Abbreviations

ADC Analogue-to-Digital Converter

DAC Digital-to-Analogue Converter

FF Fill Factor

I^2C Inter-Integrated Circuit

IC Integrated Circuit

IDE Integrated Development Environment

I_{SC} Short-circuit current

LDO Low Drop-Out

MOSFET Metal-Oxide Semiconductor Field Effect Transistor

NiCd Nickel-Cadmium

NiMH Nickel-Metal Hydride

OPV Organic Photovoltaic

RTC Real-Time Clock

SMD Surface-Mount Device

SMU Source Measurement Unit

SPI Serial Peripheral Interface

V_{OC} Open-circuit voltage

Chapter 1

Introduction

1.1 Context and motivation

This work is included in a branch of Engineering related to renewable energy, namely solar energy, encompassing the physical principles present in devices of this kind and techniques of measurement and testing of multiple characteristics. Over the last decade there has been an exponential growth of the attention given to renewable energy, which is mainly driven by two reasons: the shortage of fossil fuel, such as oil and coal, and greater environmental awareness by the general public. Renewable energies arise from this as a clean alternative to make good use of the resources of our planet.

Photovoltaic (PV) energy is based on the photovoltaic effect, converting electromagnetic radiation, typically the one coming from the Sun, in the visible range, into electricity. In the last few decades, this technology has had a notable evolution and is currently one of the most widely used renewable energy sources. The fact that sunlight is available every day for the majority of the planet makes it not only a reliable energy source, but also an interesting opportunity for new electrical applications, which do not require a constant power supply and may therefore be used away from a power socket.

The recent developments in PV devices efficiency under low-light conditions also opens up an entire new range of possibilities for indoor applications, harvesting energy from lamps and using it to power devices in various locations, without the use of cables and maybe even batteries.

The real-world performance of solar cells is essential to the understanding of its capabilities, especially in usage scenarios significantly different from those tested in a laboratory. Particularly, low-light energy harvesting is extremely dependent on module placement, orientation, light source and several other factors, which makes the assessment of the energetic potential of photovoltaic devices very delicate under these circumstances.

Beyond the research associated with photovoltaic devices, it is just as important to develop practical uses for them, so that this technology may be increasingly seen as a commercially viable energy source, which in turn fosters more research. Energy in Africa is an expensive commodity and is not taken for granted by most of the population – only about 10% of individuals has access to the electrical grid, with this percentage going as low as 2% for countries such as Ethiopia or Malawi [7] [9]. In combination with the fact that most of these countries have the highest amount of sunlight available throughout the year, this makes Africa a prime location for low cost solar applications.

Eight19 is a company based in Cambridge, United Kingdom, dedicated to the development and commercialization of organic photovoltaic cells. As the materials used are abundant in nature, the cost of production of these cells is quite low when compared to inorganic cells. Therefore, with the help and support of people at Eight19, a testing system related to real world efficiency and power output will be developed, as well as a low cost phone charging prototype circuit for rural areas in Africa.

1.2 Objectives

The objectives of this thesis are: the exploration of new applications for photovoltaic energy, as well as the potential of PV devices for energy harvesting in indoors and outdoors applications, through the development of a data logging system which measures the electrical characteristics of these devices; the experience of developing an application of this technology for possible commercial use, through the development of a low-cost phone charging platform based on solar modules. By the end of this work, I expect to not only have learned about technical and scientific topics, but also have had a significant contribution to the future, growth and success of Eight19.

1.3 Thesis structure

This document comprises 6 chapters, each of which will be briefly summarized:

- **Chapter 1:** general introduction of the scope of the thesis, context, motivation and objectives;

- **Chapter 2:** bibliographic introduction and background focused on the relevant properties of photovoltaic devices and their current applications, as well as a brief summary of the type of photovoltaic technology used at Eight19;

- **Chapter 3:** description of the development of a data logging system to be used for indoor energy harvesting assessment and exposition of results obtained from this system;
- **Chapter 4:** investigation of the potential for a low-cost phone charging system and prototype development;
- **Chapter 5:** conclusion of the project developed and recommendations for further work.

Chapter 2

Background

The generation of electrical power from a light source is known as photovoltaics and it is one of the most mainstream forms of renewable energy sources nowadays. The ability to convert radiation into electricity holds great importance, as it allows the use of sunlight to power a growing world of electronics. Furthermore, it is possible to use photovoltaics as a means to recycle artificial light in indoors scenarios.

The method through which we can harvest radiation relies on physical principles that enable the production of photovoltaic devices, better known as photovoltaic cells. A photovoltaic cell is a semiconducting device which has the ability to directly convert incident light into electricity. This conversion consists in the absorption of photons and release of energy in the form of free electrons, which may move freely through the semiconductor – this is called the photovoltaic effect. The energy of the incident light with a frequency of ν, given by $h\nu$, causes an increase in the energy of the electrons from the valence band and, if the energy is sufficient, these electrons will move to the conduction band, where they are free to move around within the semiconductor.

When a pair of semiconductors with different charge carrier concentrations (called n-type if the predominant carriers are electrons and p-type if the predominant carriers are holes) is put together, the result is a junction known as p-n junction, whose properties cause an electric potential difference between the two terminals of the device. If two electrodes are then attached to these terminals and a circuit is connected, an electric current will flow through it (see figure 2.1).

2.1 Organic photovoltaics

While photovoltaics in general has been the focus of much research since the discovery of the photovoltaic effect, the materials used until recently had been mainly inorganic semiconductors, such as silicon, which is probably the best known example of an inorganic semiconductor due to its widespread use in current electronics.

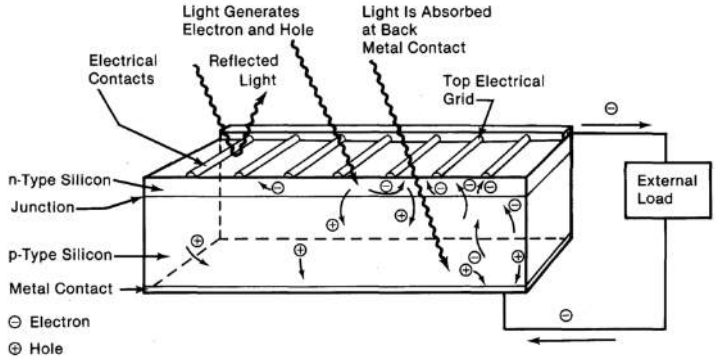

Figure 2.1: Diagram of a photovoltaic cell. Light incident on the cell creates electron-hole pairs, resulting in an electric potential difference which causes a current when connected to an external circuit [12].

Over the last 15 years, though, significant research efforts have been made in the field of organic semiconductors [4], leading to the development of what is known as organic photovoltaics (OPV). Unlike inorganic photovoltaic cells, where the main building blocks are inorganic semiconductors, in OPV cells this component is an organic semiconducting molecule, whose properties enable the realization of low-cost, large-area manufacturing techniques such as a roll-to-roll printing [17]. These materials replace the n and p-type inorganic materials with organic active layers (see figure 2.2. Some examples of currently used organic semiconductors are: phenyl-C61-butyric acid methyl ester (PCBM) and poly(3-hexylthiophene-2,5-diyl) (P3HT) [17].

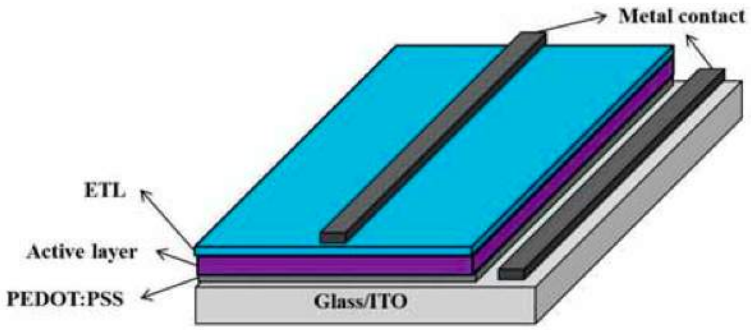

Figure 2.2: Diagram of a conventional single-junction organic photovoltaic cell. Poly(3,4-ethylenedioxythiophene) polystyrene sulfonate (PEDOT:PSS) is used as a buffer layer between the active layer and the glass / indium tin oxide (ITO). ETL is the electron transport layer [26].

Currently, the main advantages of OPV are: flexibility, as the materials used are not as fragile as inorganic semiconductors; light weight, due to the fact that plastic foil is used in its production; semi-transparency, a feature useful for covering windows with modules, for example; and good low-light performance.

Organic materials, due to their composition, are more susceptible to degradation factors such as humidity, oxygen or temperature [15]. The lifetime of an OPV cell is determined by intrinsic and extrinsic stability factors. Intrinsic instabilities are derived from the bulk of the active layer, interfaces with electrodes and the choice of electrode materials. Extrinsic instabilities arise from the sensitivity of the device to water and oxygen, which may be further enhanced by high temperature and humidity, as well as poor encapsulation [4]. The understanding and mitigation of these degradation mechanisms has had considerable attention over the years, but this still remains an obstacle in the pursuit of commercially viable OPV modules.

There is continuous research being made in this field and it is expected to continue to grow, as technology improves and allows for higher efficiency and lifetime, while keeping production costs low.

2.2 Electrical characteristics of photovoltaic cells

The photovoltaic cell (or solar cell) is the most basic application of the photovoltaic effect and the basis for larger applications of this technology. It is a two terminal device which generates an electric potential difference when illuminated, usually by sunlight. If the terminals are connected to a load, current will flow through the circuit. There are two quantities which are universally used to characterise solar cells: the open-circuit voltage, V_{OC}, and the short-circuit current, I_{SC}. As the name itself states, V_{OC} is the voltage measured across the terminals of the cell when no load is connected. If the terminals are connected together without any other elements in between, the current that flows is called the short-circuit current.

Ideally, a photovoltaic cell can be modelled as a current source in parallel with a diode. When illuminated, the source produces a current which is divided between the load and the variable resistance of the diode. The current-voltage characteristic (also known as I-V curve) of an ideal solar cell (figure 2.3) is a reflection of this model, showing the effect of load impedance on the performance of the cell; as the impedance increases, more current is drawn and the voltage tends to drop.

There are many performance parameters which can be determined from the I-V curve of a solar cell, including the aforementioned open-circuit voltage and short-circuit current. Other parameters which are widely used are the maximum power point, fill factor and efficiency. The power output of the solar cell can be calculated at any point of the I-V curve by multiplying the voltage by the

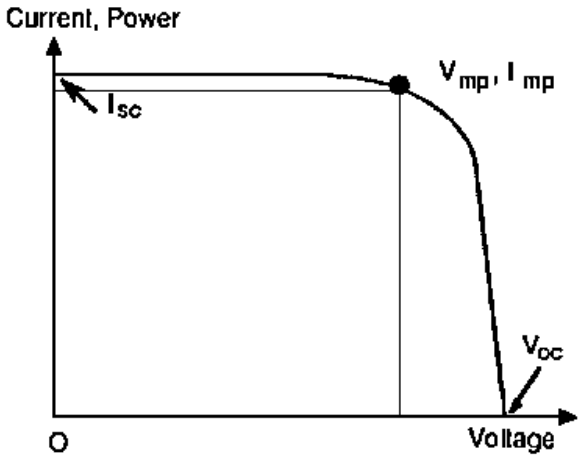

Figure 2.3: I-V curve of an ideal solar cell.

current. The point at which the power is highest is called the maximum power point. By comparing the maximum power with the expected theoretical value, the fill factor (FF) is obtained:

$$FF = \frac{P_{max}}{V_{OC} I_{SC}} \tag{2.1}$$

This quantity is commonly used as a way to assess the performance of a solar cell. Efficiency is defined as the ratio between the electrical power output of the cell and its power input.

$$\eta = \frac{P_{max}}{P_{in}} \tag{2.2}$$

The power output may be considered to be the maximum power, while the power input is the irradiance of the incident light, measured in W/m^2, multiplied by the surface area of the cell.

However, no solar cell is ideal, so it is useful to create a model which is equivalent to real world cells [25]. A shunt resistance and a series resistance are added - the resulting circuit is represented on figure 2.4. The series resistance includes the resistive contribution of the electrodes, their contact with the semiconductor and the resistivity of the semiconductor material itself; the shunt resistance arises from current leakage through the cell. The current going to the eventual load, I, is equal to:

$$I = I_L - I_D - I_{SH} \tag{2.3}$$

We may therefore conclude that the objective when manufacturing a solar cell is to make R_S as small as possible and R_{SH} as high as possible.

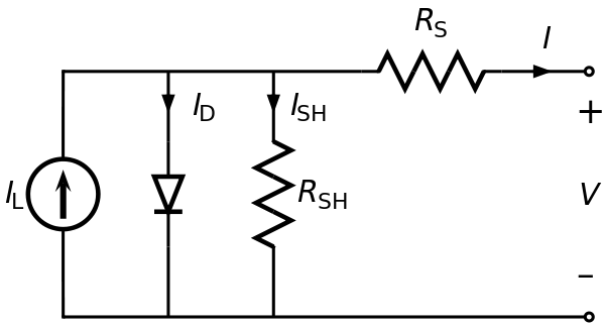

Figure 2.4: Equivalent circuit of a solar cell.

Typically, the voltage of a single cell is quite low compared to what is required for everyday applications - between 0.5 and 1.0 V. On the other hand, I_{SC} depends on the area of the cell and can be planned according to the specified requirements. To increase the voltage of the system, several cells are connected in series, constituting what is known as a module or panel. Modules may also be connected to each other in order to further increase voltage and / or current output. It is common to use bypass and blocking diodes to prevent system failure due to malfunction of a cell and also to prevent discharge from the load through the cells themselves.

2.3 Characterisation systems

The steady innovation in this area means that there is a constant need to test cells and modules, to allow a proper comparison between consecutive developments. In a lab setting, this is achieved using state of the art solar simulators and measuring equipment, allowing I-V curve tracing for different light intensities and calculations for all the different parameters previously mentioned, effectively characterising a module in a thorough way.

An example of this kind of setup is the one used at Eight19. It consists of a solar simulator, a Keithley 2400 Source Measurement Unit (SMU) and a computer running software which logs the data acquired from the SMU. The setup is represented on figure 2.5.

The solar simulator uses a lamp whose electromagnetic spectrum is close to that of the Sun and it is connected to a system which, in conjunction with a luxmeter, allows precise control over the intensity of the light that reaches the module. The SMU, as the name indicates, is capable of both sourcing and measuring at the same time; in this case, current is sourced, simulating different loads, and the voltage built up across the terminals is measured. In order to vary the intensity of the incident light, two kinds of filters may be used: mesh grids and a low-light screen. The mesh grids have different transmission coefficients, while

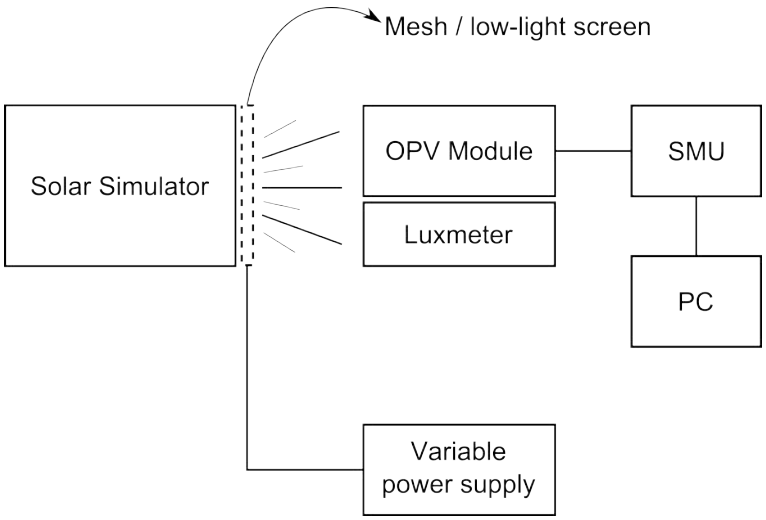

Figure 2.5: Block diagram of the solar module testing setup at Eight19.

the low-light screen is controlled using a variable power supply and allows for illuminance levels up to 1500 lux. The data collected by the SMU is transmitted to a computer running the Tracer 2 I-V curve measurement software by ReRa Solutions, which shows the I-V curve graphs and calculates I_{SC}, V_{OC}, I_{MPP}, V_{MPP}, FF and η, amongst a few other parameters (see figure 2.6).

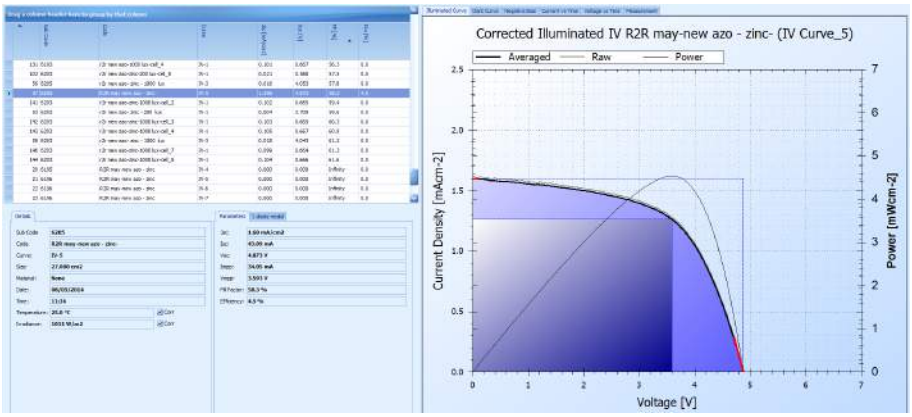

Figure 2.6: Example of the results from a measurement, as shown by the Tracer 2 software.

There is also portable equipment for this type of measurements, usually aimed at larger solar installations such as residential or industrial photovoltaic arrays. These devices use varying loads, which may be resistive, capacitive or electronic, and measure the voltage and current at each point. Field test equipment provides valuable insight into PV operation in real-world conditions and is a very useful

tool for engineers who intend to become experts on solar energy systems. However, most curve tracers have a very high cost which makes it difficult for many people to acquire one [11]. For example, the SOLAR-600 Solar Power Analyser by Amprobe is priced at roughly $1700, while the PVA-600+ PV Analyser Kit by Solmetric goes up to $4700.

2.4 Energy harvesting

Energy harvesting is the process through which energy from the environment, which would otherwise be lost, is collected and either used immediately or stored for powering all kinds of low power devices. The source of the harvested energy may be of several types: solar, wind, thermal, etc. and this field has been rapidly growing over the last few decades, mainly triggered by the desire to replace primary batteries in mobile / remote devices and supported by the technological advances in electronics and engineering in general. The energy captured in this process is generally in small amounts when compared to fossil fuels, particularly in emerging technologies such as electromagnetic or vibration energy harvesting, which means that either the power consumption of the associated system is low, or many harvesting devices are used in conjunction.

With the advent of wireless networks and low-power devices, many energy sources previously discarded as insufficient are being re-evaluated as the next generation of power supplies. Furthermore, the most prominent renewable energy sources – wind and solar – are being explored in new ways, miniaturised to fit the current technological standards.

2.4.1 Indoor light energy harvesting

Photovoltaics and energy harvesting form a great combination, as is demonstrated by the accelerating growth of solar module production over the last several years and the noticeable increase in utilisation, both in residential as well as industrial scenarios [22].

A good example of indoor energy harvesting is remote temperature measurement in different points of a factory. Combining low-power sensing and transmitting devices with small, high-efficiency, low-light optimised solar modules, it becomes possible to establish this network without the use of batteries, which have to be replaced after some time – an inconvenient process if there are dozens of devices spread throughout the site – and also without using cables, whose installation can amount to a very high cost.

Recent innovations such as NanoPower and Zero Threshold MOSFETs, by Advanced Linear Devices, which promise normal functioning using less than 1 μW of power [1], or the Energy Harvesting Wireless Sensors by EnOcean, which

allow for wireless communications using less than 1 mW of power [8], demonstrate the accompanying technological advancements of low-power systems.

There are currently energy harvesting kits on the market, available both to companies as well as to the general public. Texas Instruments manufactures and sells the EZ430-RF2500-SHE, a solar energy harvesting development kit for wireless sensor networks. It is based on a ultra low-power MSP430 microcontroller, in conjunction with a high efficiency solar panel optimised for indoors operation under fluorescent bulbs and CC2500 2.4 GHz wireless transceiver. This provides enough power to run a wireless sensor application with no additional batteries and the technical data sheet of this product includes a comprehensive application example.

2.5 Solar phone chargers

A popular consumer application of small-size solar panels is device charging, particularly phone charging. These chargers typically use crystalline silicon solar panels with a power output in the 2 - 5 W range and are frequently sold together with a lithium-ion polymer battery, ranging from capacities as low as 1000 mAh up to more than 5000 mAh. The characteristics of these chargers make them a popular item with campers or hikers, who may be spending a few days away from any sort of power supply. Their price, while not too high, still requires the user to consider whether it will be truly useful – someone who goes camping once a year might not find it a good purchase. The company Brown Dog Solar, for example, sells a USB 3 W Solar Module for $50 (figure 2.7); the addition of a battery will make the price go up to $75 or more.

In developed countries solar chargers are mostly seen as superfluous devices, something which is not actually necessary for everyday life. However, there is a very interesting market for solar chargers in developing countries, especially in Africa, where electrical energy is expensive and not available to a great part of the population, as was mentioned in the introduction to this work. The development of a low-cost solar charger might help make a difference in the lives of millions of African people and contribute to the development of their countries. Thus, this research is more focused on the available options for low-cost solar charging.

The main contribution to the overall cost of current solar modules comes from the complex and expensive processing techniques involved in crystalline silicon cell manufacturing, as it requires very tightly controlled conditions, such as high vacuum and temperatures of up to 1400 $^{\circ}C$ [2]. The use of OPV would bring these costs down and effectively make cheap, quality solar chargers possible.

A cheap solar charger was purchased from Amazon to provide an idea of what kind of products are available on the market and what quality they offer. This charger in particular cost 12£ and includes a 1100 mAh lithium-ion polymer battery. Despite claiming a 500 mA output current from the solar mod-

Figure 2.7: Example of a solar charger [5].

ule, measurements made with the Eight19 testing setup reveal an I_{MPP} of only 48 mA. Additionally, when the charger was first tested with a mobile phone, it did not work – a loose connection inside the device was found and then fixed. This shows the low quality present in the cheapest solar chargers and reinforces the possibilities available for organic solar chargers.

Chapter 3

Development of a data logger for energy harvesting assessment

Eight19 is interested in an automated system for testing solar modules under different lighting conditions, both indoors and outdoors, as a way to assess the possibilities of energy harvesting using organic photovoltaics. As a secondary objective, it would also be of interest to collect as much information about the surrounding environment as possible, in order to establish relationships between module performance and environmental conditions. For this purpose, several sensors would be used, in particular light, temperature and humidity sensors.

3.1 Methodology

3.1.1 System components planning and choice

Due to the modular nature of this system, its development requires careful planning, in order to confirm that all parts work together as expected and that there is no interference between each other. The main elements intended for the system are the following:

- OPV module;
- Microcontroller;
- Real-time clock;
- μSD card and interface;
- Light sensor;
- Temperature sensor;
- Humidity sensor;

- Power supply;
- Housing;

The following sections will take into account every important aspect to be considered in the choice for each of these elements, carefully explaining the criteria for each decision made.

Organic photovoltaic module

OPV cells and modules are characterized mainly by their I-V curves, which provide information about several parameters, such as short-circuit current, open-circuit voltage, fill factor, maximum power and efficiency. In a laboratory situation, this characterization is made using solar simulators, which accurately control the light intensity and spectrum, precision measurement apparatus and other specialised equipment, made with this specific purpose in mind. The approach made here will be quite different, with the intent to develop a highly versatile and portable system, usable in situations ranging from indoor low light to outdoor full sun, which means that the system will not be as accurate and precise as a large laboratory system.

The basic measurements to consider are short-circuit current and open-circuit voltage. Obtaining an I-V curve would require sweeping the voltage and measuring the current at each different value. Since OPV cells act as constant-current sources for the most part, a variation of load would induce a variation on voltage, which would allow the curve to be traced. A simple way to achieve this would be to use a digital-to-analogue converter (DAC) to set the voltage in incremental steps and then measure the current.

The size of the module affects the dimensioning of certain specifications and must be decided beforehand. Eight19 currently produces modules in two sizes: 27 cm^2 – mini-modules – and 320 cm^2 (figure 3.1).

The size of the mini-modules makes them better suited for the task of being placed in several different places such as walls and ceilings, so this will be the size used. Their size also means that the achievable voltage and current ranges are narrower than their larger counterparts, which simplifies the electronics required and allows for higher precision.

Microcontroller

To coordinate all the different data measurement and logging it is necessary to have a processor powerful enough for these tasks. Considering the simplicity of measuring and writing to a μSD card, the processing platform does not need to be extremely powerful or high-end; a simple yet effective option is using an Arduino board, which includes an ATMega microcontroller.

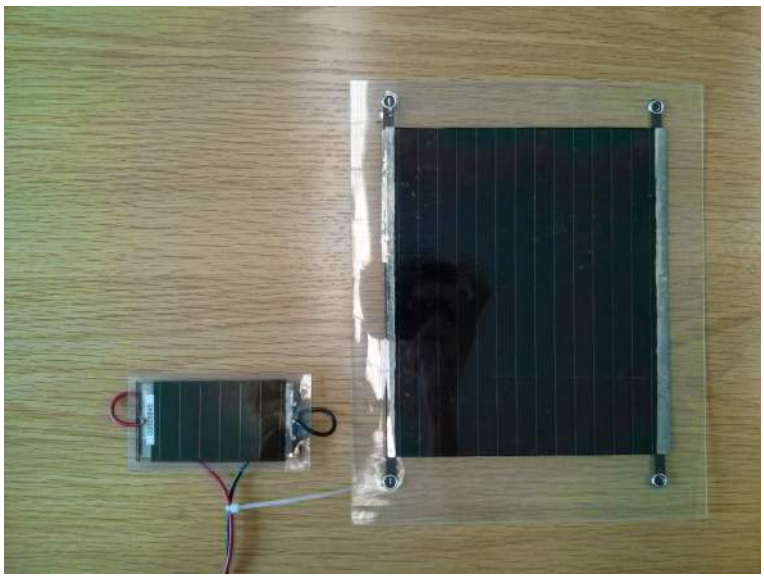

Figure 3.1: Two modules with different sizes, produced by Eight19.

The official Arduino website describes it as being "a tool for making computers that can sense and control more of the physical world than your desktop computer. It's an open-source physical computing platform based on a simple microcontroller board, and a development environment for writing software for the board" [3]. In essence, this means that Arduino boards are small, inexpensive and versatile. The fact that it is open-source makes it ideal to interface and modify according to the needs of the user and it grants access to detailed information regarding its implementation.

For this project, an Arduino-like board was used – the Seeeduino [21]. This board is based on the Arduino but adds a few key improvements, the main one being the possibility to change the logic level "HIGH" to 3.3 V instead of the 5 V on the Arduino. This allows easier interfacing with the RTC and μSD card modules, which are discussed further in the document.

In addition to the hardware, Arduino also offers a software platform which allows the programming of boards from a desktop or laptop computer – the Arduino Integrated Development Environment (IDE). This software will be essential later, in the programming stage of the project.

Real-time clock

A real-time clock (RTC) is a device used on most computers to keep track of the current time. Arduino boards only include timers, which are able to track time relative to the start of the program instructions, but do not provide information on real-time hours, minutes and seconds. An RTC module was chosen, which uses the

Inter-Integrated Circuit (I^2C) serial bus to transmit data to the microprocessor, a small lithium battery to keep the clock running and an RTC IC from Texas Instruments – BQ32000.

μSD card and interface

Once all the data is collected, the microprocessor needs to output it in a form which is easy to retrieve and keep. The way chosen for this task is the use of a μSD card, which is small, comes in various storage capacities, and interfaces easily to desktop and laptop computers. The Arduino also interfaces easily with this kind of cards, making it simple to write a text file to it containing the information required. Since the output will be a text file and considering the ubiquity of μSD cards, a common 4 GB card has more than sufficient capacity for this application.

An μSD card module was used; it is essentially a breakout board for a μSD card socket, and communication is made through Serial Peripheral Interface (SPI).

Light sensor

Accurately measuring the light intensity in the same place as the solar module allows a comparison between the measurements of the module and its known characteristics, resulting in better information regarding performance and degradation, as these are heavily dependent on light intensity. The sensor required for this should have good linearity, high precision and sensitivity and a wide rage of intensities. It is also important to take into account the spectral responsivity, temperature dependence and angular response.

Temperature sensor

The performance of an OPV cell is dependent on temperature [4], which means that measuring this variable is also of interest, although the precision need not be as high as that of the light intensity sensor. The preferred option here would be a temperature sensor IC which already contains signal processing and interface circuits, making it simple to interface with the Arduino.

Humidity sensor

Much like temperature, humidity is a parameter which has an influence on OPV cell performance and degradation [4].

Power supply

Power supply of the system may be assured either through the use of a battery or directly from a wall socket. For the purpose of making the device portable, it

is more convenient to use a battery; however, it is useful to add the option to use a wall socket, as it is more appropriate for long measurements as the ones that were taken for this work.

To power the circuit, a 2000 mAh lithium-ion polymer battery was used, providing around 3.7 V. This is not enough voltage for either the Seeeduino or the relay, requiring the use of a DC-to-DC boost (or step-up) converter. A pre-assembled circuit was acquired – the PowerPOD – providing a regulated 5 V output.

Housing

The final element to consider is the housing of the system, which should be analysed through a more mechanical perspective, as well as the requirements of the sensors used. One of the main differentiating factors between the indoor and the outdoor version of the system is the housing. For outdoor use, it is necessary to take into account the weather and climate, particularly high temperatures and rain. The challenge consists in devising a housing platform that is both waterproof and temperature resistant, dissipating heat efficiently. On the other hand, the indoor model will not be used under demanding conditions, enabling the use of low-cost, common materials.

Other components

Apart from these modules, a few more components had to be used to achieve the intended purposes: to be able to measure both V_{OC} and I_{SC}, there needs to be some way to switch between closed and open circuit, while making sure that the closed circuit is very close to a short circuit. The best way that was found to achieve this was to use a reed relay. The lowest voltage reed relay found was a 5 V DC one, which would not work with the Seeeduino working at 3.3 V. The interface between these two elements will be done using a MOSFET to drive the relay using a 3.3 V gate to source voltage.

The relay was chosen based on the specifications required: coil voltage of 5 V, SPST-NO (Single-Pole Single-Throw Normally-Open). To switch the relay, a MOSFET (Fairchild Semiconductor 2N7000) is used in a switching configuration, allowing digital control of the switching circuit using the Seeeduino.

It will also be necessary to use two operational amplifiers for V_{OC} and I_{SC} measurement, as is explained in the "Circuit development" section. The model chosen for both was the MCP6291 by Microchip, which is single-supply (5 V), draws only 1 mA of quiescent current and has an input impedance of $10^{13}\,\Omega$, with a gain-bandwidth product of 10 MHz. Considering the amount of operational amplifiers available on the market, it is probable that there others which are better suited for this application; however, this is merely a prototype and the

main point is that it is functional; a final version would require a more thorough research.

A complete list of components can be found in Appendix A.

3.1.2 Light sources

When using OPV modules or other light-dependent devices, it is essential to understand the sources of electromagnetic radiation present in the environment. As was mentioned before, this system is to be used in an indoor low-light setting; however, the objective of this analysis is to make it as close to real-world conditions as possible, so natural sunlight will also be present in the testing area.

It is important to define here two measures associated with light intensity: irradiance and illuminance. Irradiance is a radiometric quantity and is equal to the power of electromagnetic radiation per unit area incident on a surface – it is measured in W/m^2. Illuminance is a photometric quantity equal to the total luminous flux per unit area incident on a surface – it is measured in lux (lm/m^2). The difference between these two quantities is that irradiance is a general measure of light intensity for all wavelengths, while illuminance takes into account the varying sensitivity of the human eye to different wavelengths. Illuminance can be derived from irradiance by using the luminosity function to convert from watt to lumen [23].

3.2 Circuit development

As a way to explore the potential of OPV modules in low-light energy harvesting scenarios, the indoor version of the system was chosen as a priority; this section concerns the development of this system. The requested essential characteristics of the system were:

- V_{OC} measurement;
- I_{SC} measurement;
- Capability to accept different solar modules;
- Portable and easy to carry.

The first step consisted of figuring out the most accurate way to measure V_{OC} and I_{SC}. V_{OC} measurement is fairly straightforward, as the Seeeduino board has analogue inputs which measure voltage between 0 and 3.3 V. The solar module is connected in reverse because, much like a photodiode, the current generated is a reverse current. Due to the solar module being connected in reverse (positive

terminal to ground), an inverting op-amp configuration had to be used to allow the Seeeduino to read the voltages (figure 3.2).

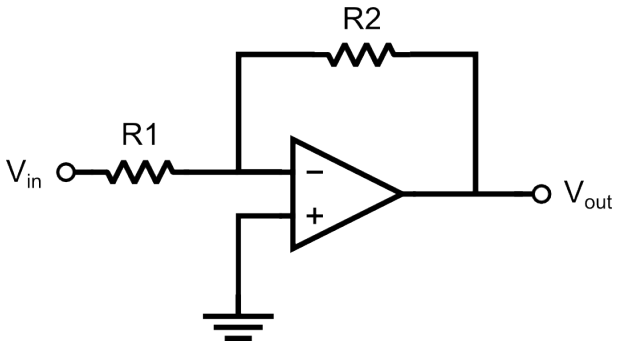

Figure 3.2: Schematic of an inverting amplifier.

The gain of this amplifier is given by:

$$A_v = \frac{V_{out}}{V_{in}} = -\frac{R2}{R1} \tag{3.1}$$

The voltage of the OPV modules used for this application is a bit less than 5 V at 1 sun, so the gain was set to -0.65.

Several options were researched for I_{SC} measurement, ultimately narrowing it down to two: using a current-sense (shunt) resistor, the same way it is done in digital multimeters; or using a transimpedance amplifier, an op-amp based circuit which acts as a current to voltage converter (figure 3.3).

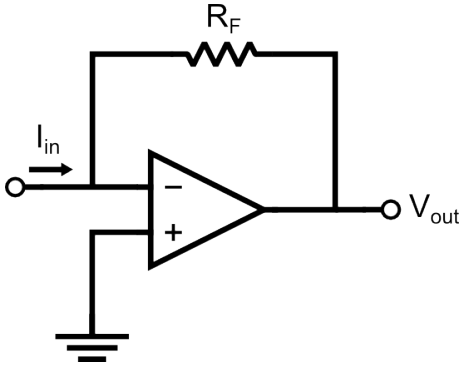

Figure 3.3: Schematic of a transimpedance amplifier.

According to a technical paper by National Instruments [20], the transimpedance amplifier (referred to as "feedback ammeter") is a better solution for measurements in the μA, nA and pA range. Considering that the maximum output of

the mini-modules under indoor light conditions is no more than 10 mA and lower values in the μA range will be common, this was decided as being the best option. The relationship between the input current and the output voltage is:

$$\frac{V_{out}}{I_{in}} = -R_F \tag{3.2}$$

Considering the upper limit of the current range – 10 mA –, R_F was set to 330 Ω to allow for the use of the entire input range of the Seeeduino.

The schematic of the full circuit is represented on image 3.4. The analogue ports on the Seeeduino are represented by the code "A", while the digital ports are represented by the code "D". On the μSD card module, the acronyms SS (Slave Select), MISO (Master In Slave Out), MOSI (Master Out Slave In) and SCK (Serial Clock) refer to the logic signals specified by the SPI bus for device communication. The SDA (Serial Data) and SCL (Serial Clock) on the RTC module represent the communication lines of the I^2C interface.

	Nominal value (Ω)	Measured value (Ω)
R1	2×10^6	1.985×10^6
R2	1.3×10^6	1.289×10^6
R3	330	327

Table 3.1: Measured values of the resistors used on the amplifiers.

The resistors used on the amplifiers were measured using a standard multimeter and their real values are presented on table 3.1. From these values it is possible to determine the real approximate values of the gain – -0.649 for the inverting amplifier and -0.327 for the transimpedance amplifier.

3.2.1 Testing and calibration

After having all the components, the circuit was assembled on a breadboard for testing and calibration purposes. Firstly, voltages were measured at key points of the circuit – mainly at the outputs and supply of the op-amps and relay. Then, the whole circuit was calibrated using a Keithley 2400 SMU. By applying different voltages and currents to the inputs, the outputs were measured and two calibration lines were obtained from the data (figures 3.5 and 3.6). The fit parameters given by the gnuplot software are the following:

Voltage:

- $m = -0.6511 \pm 0.0001\ mV/mV$
- $b = -2.643 \pm 0.200\ mV$

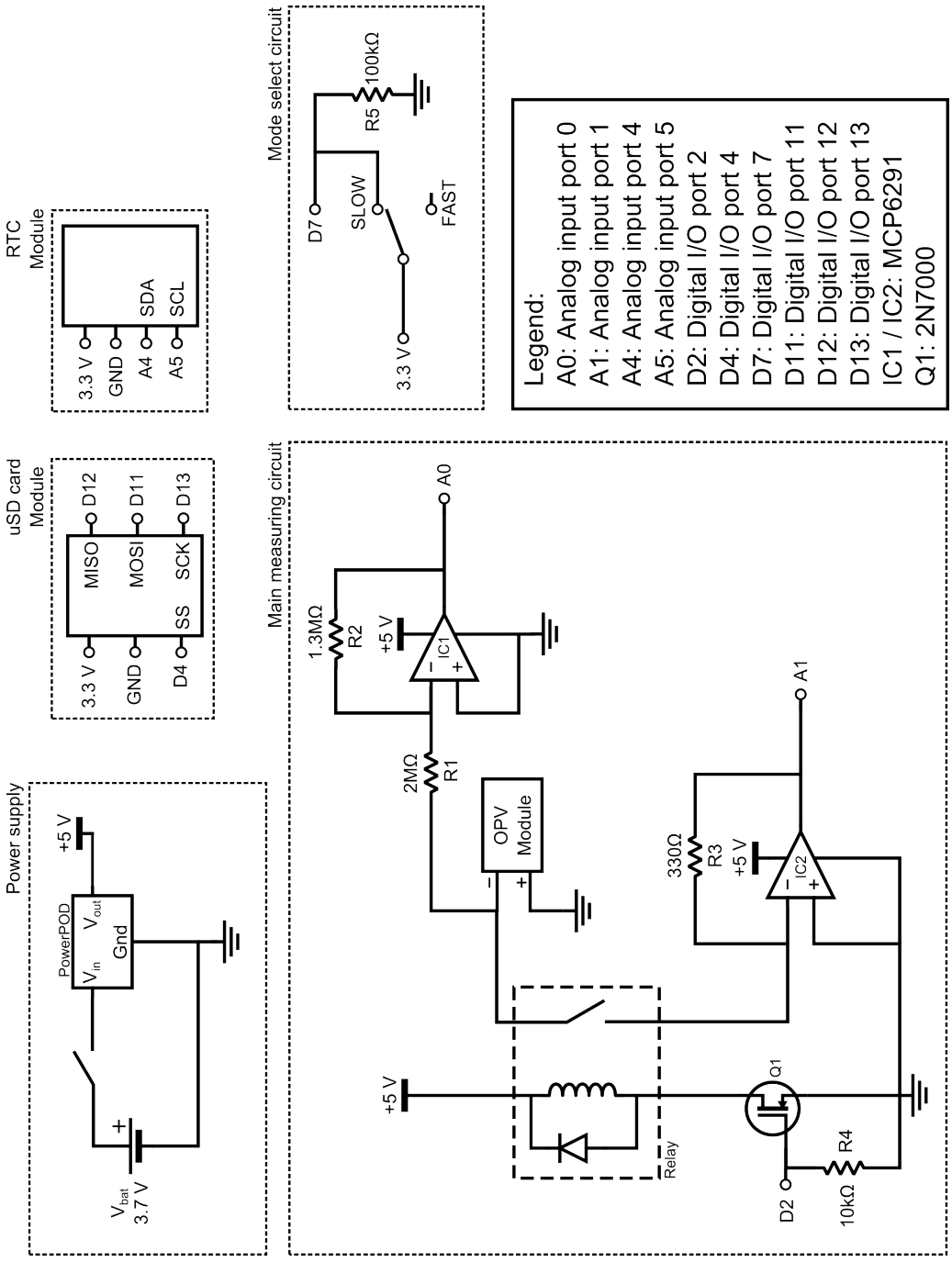

Figure 3.4: Schematic of the circuit for the prototype of the data logger.

Current:

- $m = -0.3277 \pm 0.0001\ V/mA$
- $b = 0.302 \pm 0.200\ mV$

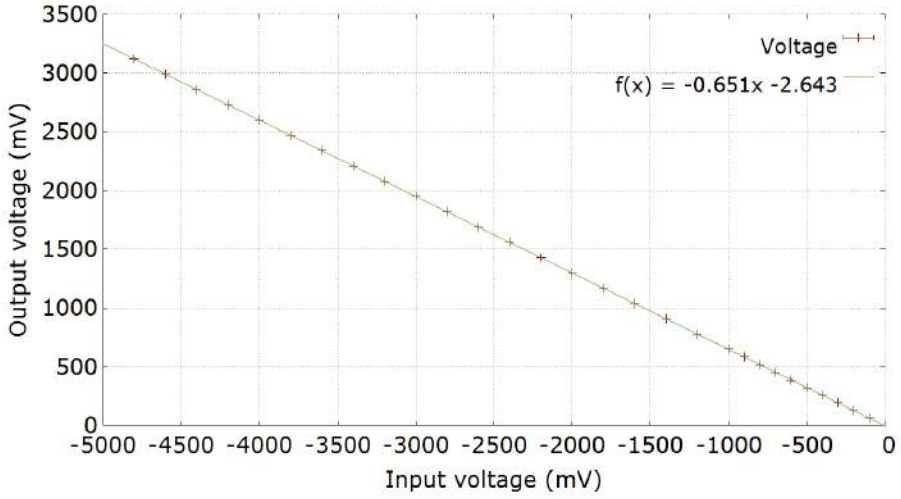

Figure 3.5: Calibration of voltage measuring circuit. Both x and y error bars are present, yet too small to be visible.

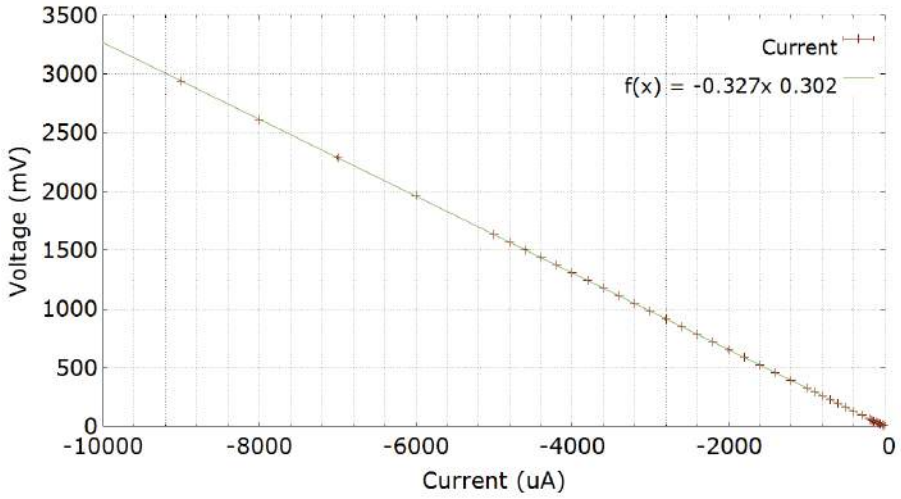

Figure 3.6: Calibration of current measuring circuit. Both x and y error bars are present, yet too small to be visible.

These lines are essential to the project, as they provide a way to accurately evaluate the results obtained, and will be inserted into the software which will be running on the Seeeduino board.

The initial measurements revealed some discrepancies between the values obtained and those measured using a multimeter. Upon further inspection, a problem was found in which the voltage of the photovoltaic cell dropped a few hundred millivolts from what was expected as V_{OC}, when in contact with the circuit. Due to the characteristics of PV cells, a current draw will place the voltage at a certain point in the I-V curve of the cell - the higher the current, the lower the voltage. The impedance seen by the cell is the input impedance of the inverting amplifier, which in this case is equal to the value of resistor R1. Since the cell used outputs very low power, the resistor used has a value which is too low, drawing too much current and causing the voltage to drop. This was also causing some current to flow through the inverting amplifier while measuring current, instead of having the majority of the current going into the transimpedance amplifier. This problem was solved by replacing the inverting amplifier resistors with higher value ones, while keeping the same gain - 2 $M\Omega$ and 1.3 $M\Omega$ instead of 20 $k\Omega$ and 13 $k\Omega$, respectively. This circuit was tested and the values measured were now very close to V_{OC} and I_{SC}.

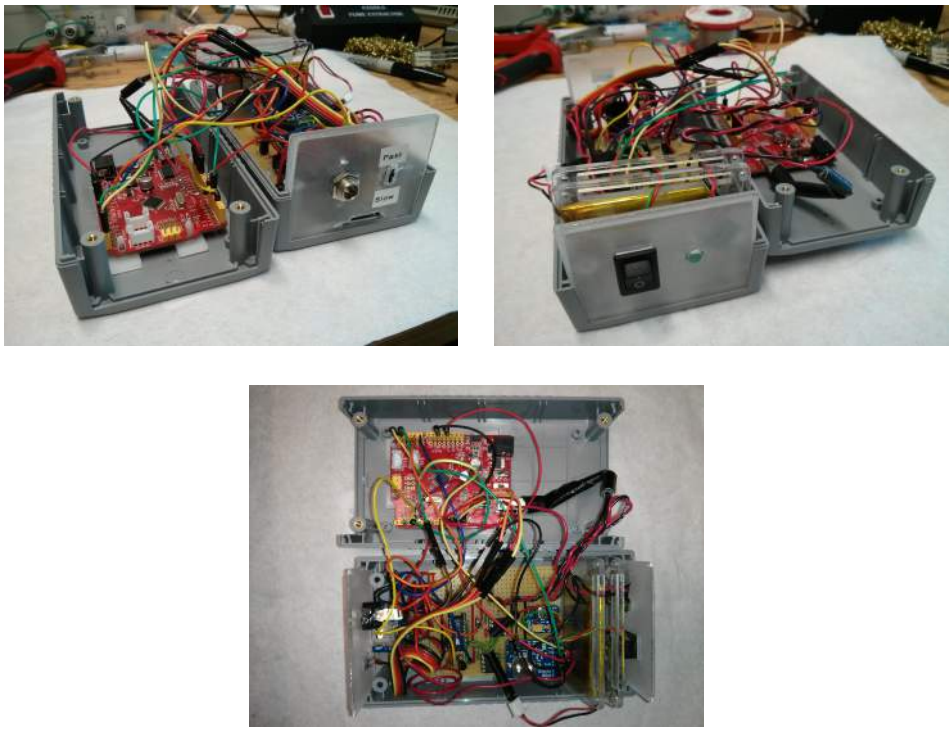

Figure 3.7: Photos of the data logger.

With the whole system characterized and functional, the circuit was soldered on to a stripboard, being careful to make it as modular as possible, to allow for modifications and improvements. Finally, all the elements of the system were mounted in a plastic case (see figure 3.7) and acrylic plates were cut to fit the case and allow for external access to the μSD card and OPV module plug. Two switches were added, one for power (on/off) and another for changing data collection modes: "fast", for intervals of 0.5 seconds between measurements and "slow", for intervals of 5 seconds. An LED was also added to indicate that the unit is working.

The Seeeduino code, which may be seen on Appendix A, uses a few open-source libraries which implement different functions of communication with the μSD card and RTC module, as well as providing a sleep mode for power savings. The output of the programme to the μSD card is a .txt file with 4 columns: timestamp, time, voltage and current. The timestamp provides the real-time information from the clock, while the time column gives a rough idea of the interval between measurements, which is useful for making graphs.

The omission of the sensors discussed in the previous section was deliberate, as these are not essential for the proper functioning of the system; this matter is more thoroughly approached in the final chapter.

3.3 Results and analysis

To demonstrate the use of this system in a strictly indoors setting, a windowless room was used, in which a single fluorescent lamp was present. This lamp in particular is model MCFE 100W/25 by Philips, with a color temperature of 3500 K. Using a calibrated luxmeter and a measuring tape, the illuminance levels were measured in several positions along a vertical axis; the data logger was used to measure V_{OC} and I_{SC}. To obtain the power density from V_{OC} and I_{SC}, the definition of fill factor is used:

$$FF = \frac{P_{max}}{V_{OC} I_{SC}} \implies P_d = \frac{V_{OC} I_{SC} FF}{A} \quad (\mu W/cm^2) \tag{3.3}$$

The value used for the fill factor was 33.8 %, which was obtained from measurements done on the laboratory testing setup, while the active area of the module, A, is 27 cm^2. The results are can be seen on figures 3.8 and 3.9.

A linear relationship between power density and illuminance is observable and it provides valuable information about the possibilities for indoor energy harvesting. For example, a small $10cm \times 10cm$ module placed 10 cm away from a fluorescent lamp would provide a bit more than 2 mW of power, which could be paired up with a low-power sensor for an energy management application.

To provide results from another type of environment, involving a mixture of artificial and natural light, an experimental setup was created to test the system

under different circumstances, which can be compared between themselves. The setup consisted of a small room (4.5 × 3.5 × 2.5 m), with a large window facing West and three fluorescent lamps on the ceiling. Several positions were then chosen, on which the OPV module would be placed for a set amount of time, mainly as a way to obtain data on the influence of the weather conditions and

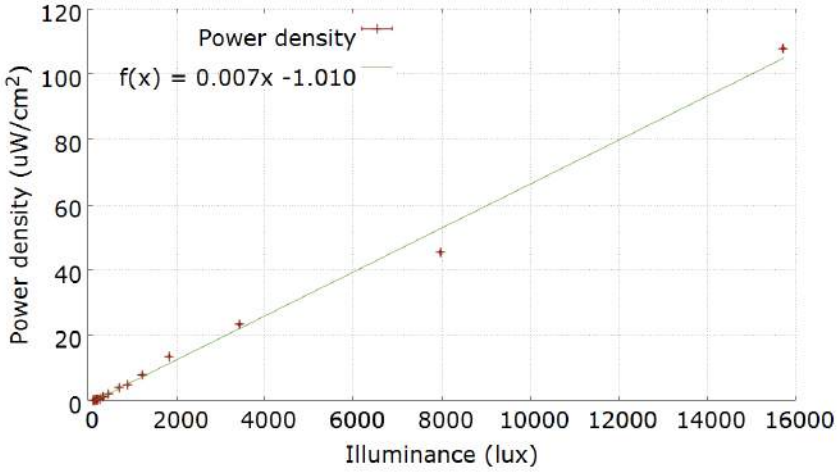

Figure 3.8: Variation of power density from solar module with illuminance levels from a fluorescent lamp. Both x and y error bars are present, yet too small to be visible.

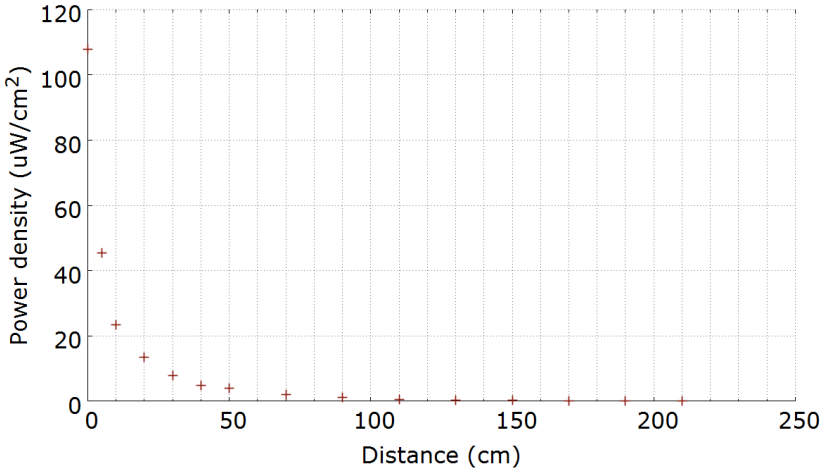

Figure 3.9: Variation of power density from solar module with distance from a fluorescent lamp.

also to try to estimate the total amount of energy available for harvesting. As may be seen on figure 3.10, the positions were selected so as to allow for some diversity in measurements:

1. Ceiling
2. North-west wall
3. South-east wall
4. North-east wall
5. Window (South-west)

A few other sets of measurements were also made, as a way to compare smaller differences around a certain spot, such as on a smoke detector, facing different directions and directly facing a fluorescent lamp, with the blinds closed.

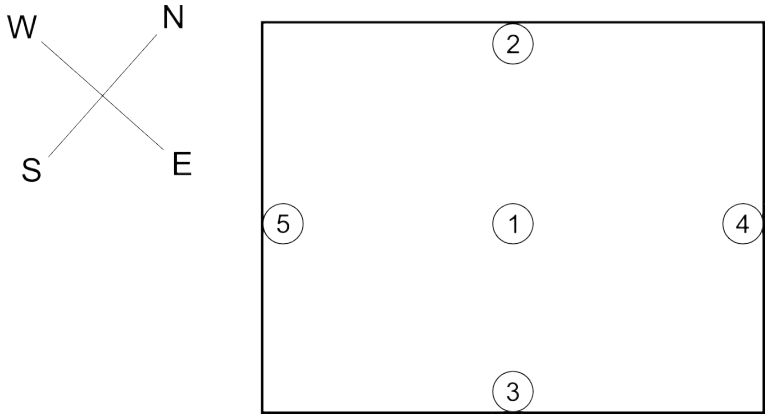

Figure 3.10: Diagram of the room and selected positions.

The results from the smoke detector measurements represent a scenario where one might use a small solar module to power one of these devices or others, such as sensors. As can be seen on table 3.2, daylight has a great influence on power output of the module; however, it is still significantly lower than what is usually required for the applications mentioned. Nonetheless, in conjunction with a battery this could provide a viable solution: e.g. a wireless sensor which only needs to transmit information every 10 minutes. The energy harvested during the 10 minutes in which the system is sleeping could be stored and used for the transmission.

The measurements taken on the other positions in the room were taken over the course of 24 hours and can be seen on figures 3.11 through 3.15. The results can be integrated to give a rough estimate of the total energy which is possible to collect over the time period, using the formula:

Orientation	Luminosity (lux)	V_{OC} (mV)	I_{SC} (μA)	Power ($\mu W/cm^2$)
Down	360	1756.3	24.2	0.79
Window (SW)	415	1942.4	51.7	1.86
North-west	190	1696.0	21.4	0.67
North-east	140	1509.9	9.7	0.27
South-east	200	1727.4	19.5	0.63

Table 3.2: Results of the measurements on the smoke detector.

$$E_d = \frac{\sum_{i=1}^{n} {P_d}^i}{24n \times 1000} \quad (mWh/cm^2) \tag{3.4}$$

where P_d^i is the power density obtained from the data and n is the number of data points collected.

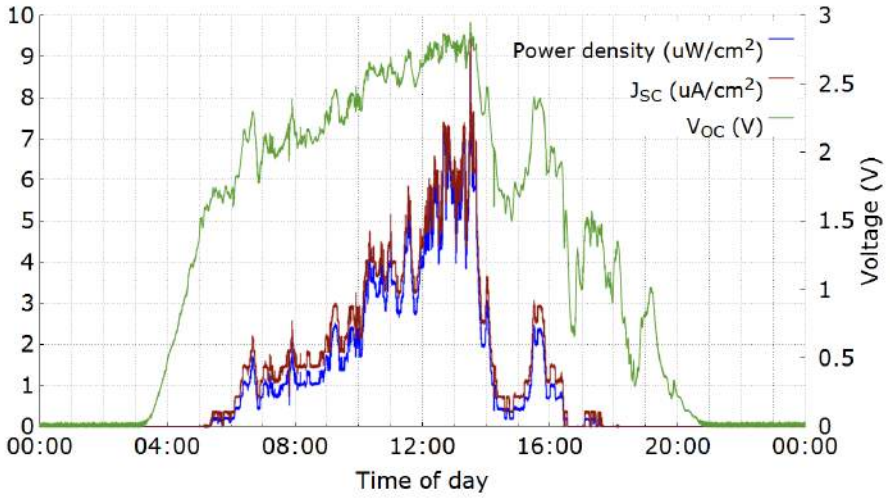

Figure 3.11: Results of the measurements taken on the ceiling.

As expected, there is generally a much smaller variation in voltage than in current, which explains the fact that the power output of the module follows the current curve more closely. The influence of the weather is clearly very significant, as can be observed in the graph from figure 3.13, for example, where there is a large power drop at about 16:30, which coincides with a rainstorm that brought very dark clouds; about 30 minutes later, the sky cleared up again.

Table 3.3 shows the total approximate amount of energy collected over the course of each of the days represented in the previous graphs. As expected, when the module is placed on the window facing the outside, the amount of energy received is much higher due to the energy that comes from the Sun.

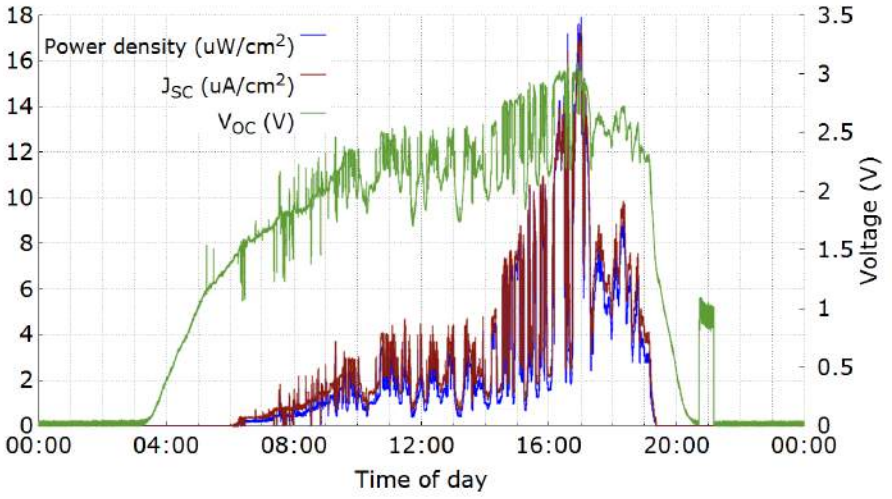

Figure 3.12: Results of the measurements taken on the north-west wall.

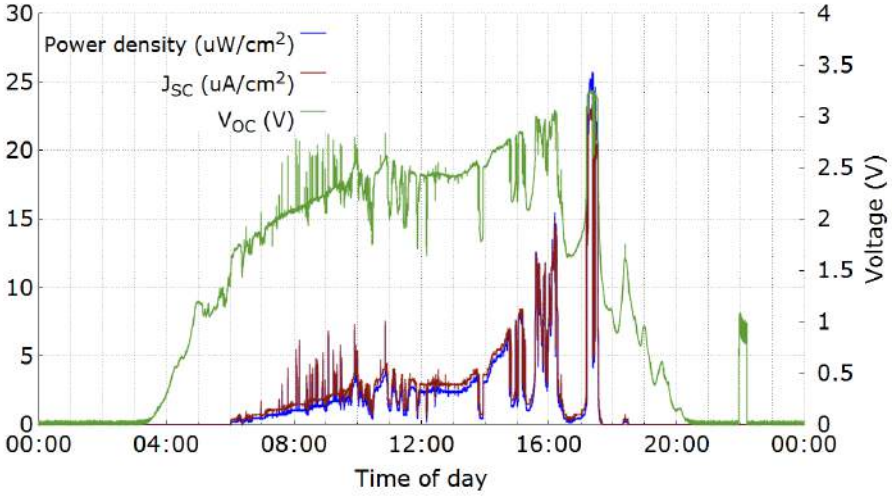

Figure 3.13: Results of the measurements taken on the north-east wall.

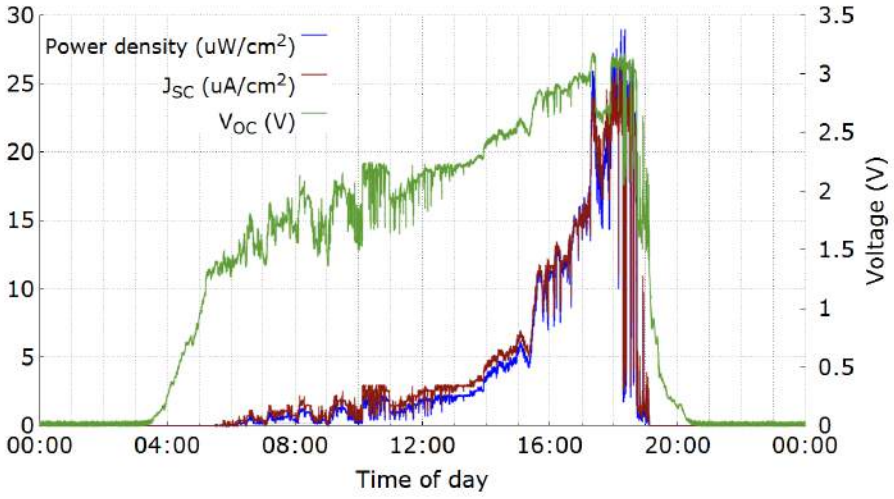

Figure 3.14: Results of the measurements taken on the south-east wall.

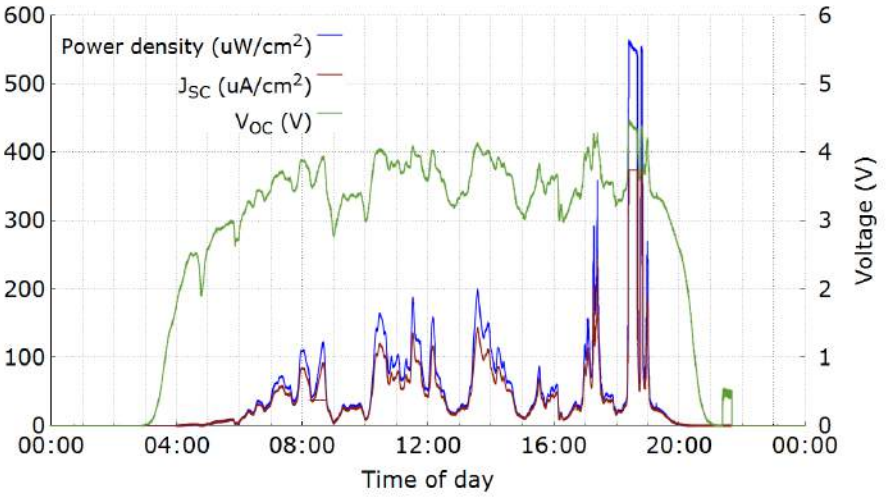

Figure 3.15: Results of the measurements taken on the window, facing outwards.

Position	Total energy (μWh)
Ceiling	656.23
North-west wall	851.95
North-east wall	910.71
South-east wall	1871.12
Window wall	22551.05

Table 3.3: Total energy collected over the course of a day for different positions.

Chapter 4

Development of electronics for phone charging

One possible application that Eight19 is interested in is phone charging from an OPV module, mainly as a way to reach off-grid communities whose alternative to phone charging is going to a dedicated "charging station", which is neither convenient nor cheap. According to an Eight19 source in Kampala, Uganda, "phone charging demand is close to lighting demand in Africa. People prefer to have their phones charged and they normally pay money for that. It is usually around 0.2 USD for every time they charge. Some rural entrepreneurs have purchased solar systems and are able to charge up to 15 phones in a day". To put things in perspective, the World Bank estimates the global national income per capita in Uganda to be 480 USD [9], which yields a monthly income of 40 USD. It is therefore important to reduce the cost as much as possible and this will have an impact not only on the planning of the whole circuit, but also on component choice, as well as dimensioning of OPV modules. Several options will be explored, such as the use of batteries for energy storage and the effects of different kinds of components on efficiency, along with a cost comparison for the different alternatives.

4.1 Methodology

4.1.1 Power requirements for phone charging

It is first important to assess the power requirements of the project and the suitability of Eight19's modules for this application by determining essential factors, mainly the voltage and current required. The main point is to develop a charger which is as universal as possible, i.e., which may be used with many different phones particularly in the low price range, as these are most common amongst populations in Africa. For a few years now, there has been a rise in the

number of phones which connect to a USB interface and allow charging, making this the ideal platform to develop the charger on. Universal Serial Bus (USB) is an industry standard designed for easier peripheral interface, which defines connectors and communication protocols used for connection between computers and external devices. According to the USB Implementers Forum, Inc., a non-profit corporation formed to provide a support organization and forum for the advancement and adoption of USB technology, the USB 2.0 specification allows for device charging up to 500 mA at 5.00 ± 0.25 V [13], while version 3.0 allows up to 900 mA charging current at 5.00 ± 0.25-0.55 V [14]. This means that the phone charging voltage we should be aiming for is 5 V. The current is dependent on the specifications of the solar module used. However, considering that cost is essential, as well as size, it is important to understand the effects of low currents on the charging circuit. For this purpose, a Nokia C1 phone was purchased, as it reflects the type of phones used in the target market. Since no literature was found on the subject, this was done empirically, by applying diminishing current values until the phone stopped charging. With the phone charging through a USB port, the current draw is 420 mA; this will be the starting point for the tests. Both the wall charger and the USB port are rated at 5 V, so we should assume that this is the optimal charging voltage and will keep it around this value. After making the measurements, the minimum charging current was found to be around 100 mA; below this point, the power consumption exceeds the power provided and the phone charges intermittently, possibly due to the power consumption of the screen, as it turns on when the phone begins charging.

4.1.2 Energy storage

One essential aspect to consider is the usage or not of energy storage devices – batteries. There are two main points to consider here: cost and convenience. Obviously, the use of batteries raises the cost of the whole system, not only because of the batteries themselves, but also for the extra components needed for power management, such as battery charge controllers. Nonetheless, solar panels can be quite sensitive in terms of their power output, sometimes requiring only a small rotation to completely change the current provided. Adding a battery helps to mitigate this problem by keeping some energy on hold for eventual drops in power output. This also brings the added benefit of allowing a user to disconnect the solar panel from the phone during the day and charge the phone from the battery at night. Both these options will be further explored and discussed here.

Direct phone charging

Direct charging is what will be defined as charging without any means for energy storage. This is the cheapest form of charging as it only requires a solar panel and a few common components. The panel can be made to the intended specification,

but its open-circuit voltage needs to be between around 6 V and 10 V, depending on number of photovoltaic cells and material used. From the measurements made it was concluded that the phone used only charges when the input voltage is above 4.7 V. The maximum limit was not tested due to safety concerns, but since 5.25 V is the maximum output voltage of the USB standard, it is safe to assume that voltages higher than 5.25 V will not charge the phone and may possibly cause damage.

Figure 4.1 shows maximum power point voltage measurements done on the Eight19 solar simulator, under irradiance levels going from around 10 W/m^2 up to almost 1000 W/m^2; for irradiance levesl between 100 and 1000 W/m^2, the maximum variation is about 50 mV, with an average of 590 mV / cell. If a 9-cell module is produced and a low forward voltage diode is placed in series between the module and a phone, it should meet the power requirements previously determined.

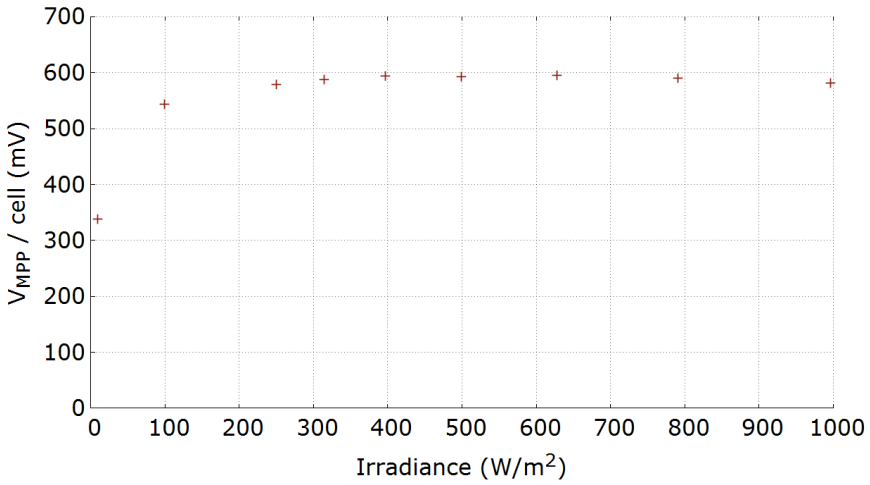

Figure 4.1: Variation of maximum power point voltage per OPV cell for different levels of irradiation.

If this is not achievable, the narrow window of charging voltage means that the solution is to use a component such as a voltage regulator, preferably a low-dropout (LDO) regulator, to keep the voltage around 5 V. An LDO regulator is a linear voltage regulator which can operate with a very small difference between input and output voltage; these also tend to be more efficient and dissipate less heat. An even more efficient alternative is a DC-to-DC step-down converter, which uses capacitors and inductors to store unused energy and is especially advantageous in large output to input voltage differences.

With direct charging comes the possibility of charging other devices other than mobile phones, such as flash lights or other USB-powered devices. Therefore, the

usage of a low forward voltage blocking diode is important to prevent any kind of discharge through the module itself. A particular class of devices which is interesting to discuss is power banks. These stand-alone batteries are offered in a wide range of capacities and are increasingly popular as consumer products, which means that their prices have been dropping significantly, posing as competition for the energy storage devices proposed below. Three of these power banks were purchased to determine whether they would work properly with the prototypes developed. Using a power supply, the minimum charging current was determined – all of the power banks charged down to less than 5 mA, which confirms that they should work properly with the prototypes developed.

Phone charging via batteries

We will refer to phone charging via batteries as a way of charging which makes use of an energy storage device, more specifically one or more batteries. The advantages of energy storage were explained above and are important enough not to be dismissed. Within the field of batteries there is a lot of variety, though it is best to stick to the most common ones as they are easier to find and are generally cheaper. The main points to consider when choosing a battery are:

- Capacity
- Voltage
- Technology

Capacity is defined as the amount of electric charge a battery can deliver at a specified voltage and is usually given in units of milliamp-hour (mAh); a related quantity frequently used is the energy, measured in watt-hour (Wh). For the purpose of this project, a capacity which is at least equal to that of the phone is required, as rechargeable batteries should not be discharged at a rate higher than 1C, for prolonged battery life and overall safety. The C-rate is the rate of charge (or discharge) compared to the capacity of the battery:

$$C_{rate} = \frac{charge/discharge\ current}{capacity} \tag{4.1}$$

For example, a 2000 mAh battery discharging at a 1C rate would be sourcing a current of 2000 mA; at a rate of 0.5C, the current would be 1000 mA. Since the maximum charging current for safe battery operation is also 1C, it is clear that the minimum battery capacity should be at least equal to that of the phone.

Regarding voltage, this parameter is mostly dependent on two things: solar panel voltage and phone charging voltage. On one hand, the voltage provided by the panel must be higher than that of the battery, otherwise it would not charge. On the other hand, it has been demonstrated that the voltage for charging a

phone should be approximately equal to 5 V. The ideal setup would then be a 5 V battery; however, these are not very common and therefore cost quite more than other kinds of batteries, which have lower voltages. A possible solution is to use a DC-to-DC converter, a circuit which converts a DC source from one voltage level to another.

Finally, the technology used in the battery is important because it determines certain characteristics such as total battery lifetime or the presence of memory effect. For rechargeable batteries, the most common technologies nowadays are lead-acid, nickel cadmium (NiCd), Nickel Metal Hydride (NiMH), and lithium-ion polymer. Lead-acid batteries are mostly used in automotive applications due to their ability to support high surge currents; for this application, they are not indicated as their energy to weight ratio is low compared to other technologies. This leaves NiCd, NiMH and lithium-based batteries. NiCd is the technology used in old mobile phones and suffers from memory effect, which is something to avoid considering there are other alternatives.

NiMH batteries are technologically similar to NiCd batteries, with the advantages of having higher energy density and no memory effect, as well as not containing any toxic metals. They come in standard battery sizes, such as AA and AAA, and capacities are in the same range as lithium-based batteries – 100 mAh to 2000+ mAh. Their main disadvantage is the high rate of self-discharge (although there are currently more expensive versions with low self-discharge), losing up to 30% of capacity over a month, versus around 10% for lithium-based batteries. However, they are also significantly less expensive than lithium batteries, which is an essential point for this application.

Due to the law of conservation of energy, the power consumed by a certain load can never be higher than what is supplied by a battery. Therefore, the use of a DC-to-DC converter to reach a higher output voltage always results in a decrease in current output. Considering the voltage required in this case is 5 V, the efficiency of the circuit is directly related to the voltage of the battery – lower voltage implies lower efficiency, as more current is wasted on the converter. Therefore, it is best to consider only voltages closer to 5 V. As a way to evaluate several options, three prototypes involving energy storage will be developed: 3-battery NiMH (3.6 V), 4-battery NiMH (4.8 V) and single-cell lithium-polymer (3.7 V).

4.1.3 Available solar energy

An essential part of this project is to assess the total amount of solar energy which can be collected throughout a certain period of time. In order to achieve this, we need to take into account several factors, such as:

- Available energy from the Sun;
- Conversion efficiency of module;

- User behaviour / exposure to sunlight;

Each of these topics will be discussed in detail, so that they can be combined and an estimate of the total available energy can be determined.

Solar irradiance is usually given in terms of power per unit area (typically kW/m^2) and is a measure of the irradiance produced by the Sun. Another unit of measurement associated with solar energy is insolation, defined as the energy received on a given surface during a given time (Wh/m^2). The values of these quantities are very dependent on the position of the area of interest and also on time of the day and year.

The Institute for Energy and Transport, which is part of the Joint Research Centre of the European Commission, has an information system which provides a map-based inventory of solar energy resources in Europe, Africa and South-west Asia – PVGIS (Photovoltaic Geographical Information System) [10]. The PVGIS database includes both geographical and climatic data, containing daily irradiation. This is more useful than calculated values, as it takes into account the influence of weather changes. Using the data available, the range of power output was calculated for different regions, depending on the time of year, hour of day, and size of solar panel. From the global irradiation data we can calculate the power output of a solar panel, based on its size and efficiency:

$$P = \frac{\eta G A}{10} \quad (mW) \tag{4.2}$$

with η being the efficiency, G the global irradiance (on a fixed plane) in W/m^2, and A the area of the panel in cm^2. The efficiency considered was 3% and the areas were approximately those corresponding to the one-sun maximum output of 200, 500, 1000 and 2000 mW – 100, 200, 400, and 800 cm2, respectively. One-sun maximum refers to a solar irradiance of 1000 W/m^2. Considering the connections that Eight19 has to Kampala, Uganda, this place was chosen as example and two months were considered, January and July, which represent the peak of summer and winter, respectively. The data obtained, as well as the calculated power output, is represented on figures 4.2 and 4.3.

According to the research done for section 4.1.1, the minimum power required for direct phone charging is 500 mW (100 mA at 5 V). If we look at the data obtained and calculated, it is clear that, for Kampala, a 1 Wp (Watt-peak, the highest power that a solar module can output) solar panel (400 cm^2) would be sufficient for direct charging and in fact should be able to provide a full charge for our model phone, with its 800 mAh battery – at 3.7 V, the total energy of the battery is 2.96 Wh. On the other hand, a full day of sunlight may provide between 6500 and 7200 mWh, which is enough energy to charge our model phone at least twice.

In order to provide a better understanding of the effect of solar module area on total energy available, some calculations were made to estimate the total amount

of energy available for collection, whose results may be seen on figure 4.4. For each value of module area, the power for each time of day (using the irradiation data represented on figure 4.2) was calculated using the previously mentioned equation:

$$P = \frac{\eta G A}{10} \quad (mW) \tag{4.3}$$

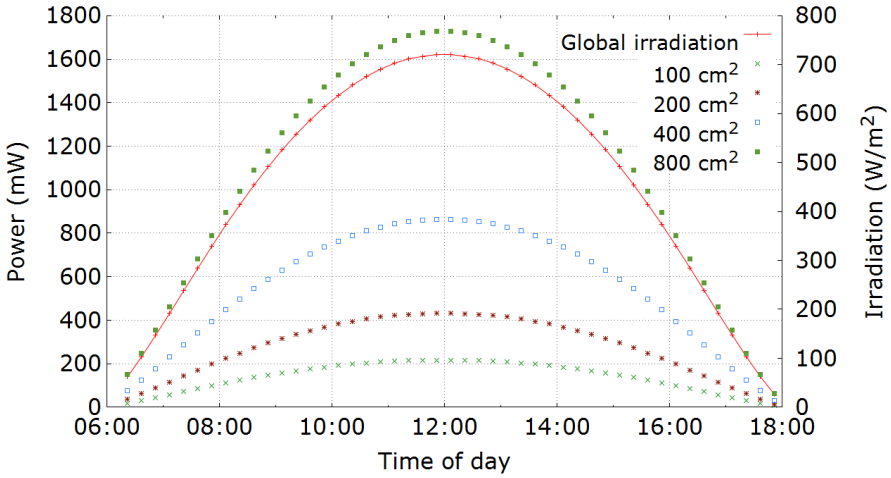

Figure 4.2: Irradiation data obtained (July) and calculated power output of solar modules for different sizes, at 3% efficiency.

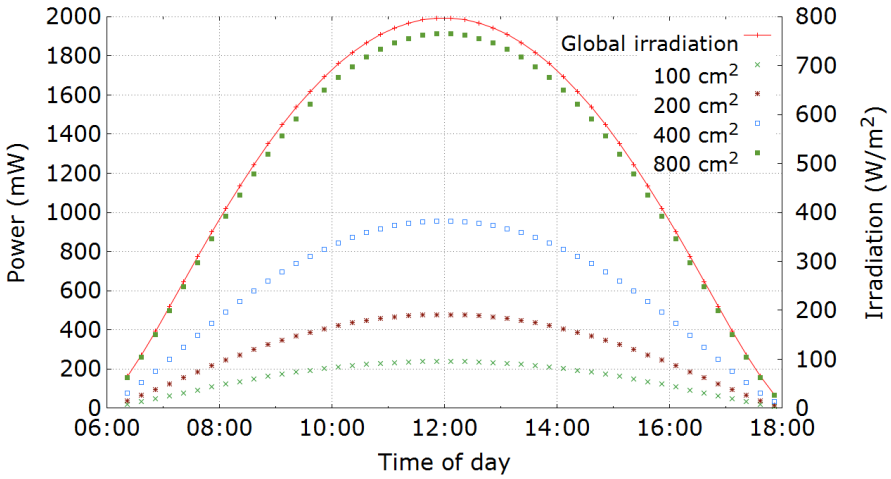

Figure 4.3: Irradiation data obtained (January) and calculated power output of solar modules for different sizes, at 3% efficiency.

Then, the resulting values which are above 500 mW are summed and from this sum it is possible to obtain the total amount of energy collected (the division by 4 is due to the fact that there are four measurements per hour – this way the result comes in mWh):

$$E = \frac{\sum_{i=1}^{n} P_i}{4} \quad (mWh) \tag{4.4}$$

There are two effects occurring here: on the one hand, the larger the area the higher the amount of time that the module output is above the threshold of 500 mW; on the other hand, this also means that there is more energy collected during the same amount of time. Estimates for 5% and 10% efficiency were also made, as a way to evaluate some more long-term applications for Eight19's technology.

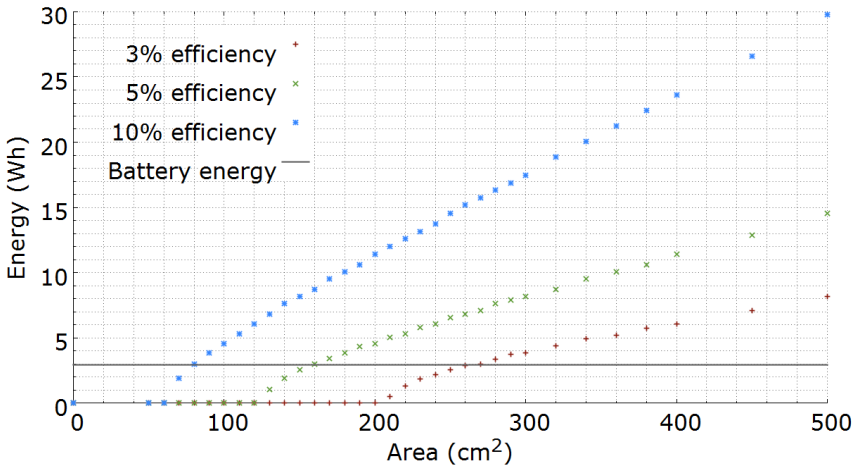

Figure 4.4: Maximum total energy collected in a day as a function of solar module area for different efficiencies. The horizontal line represents the total energy of a 800 mAh battery working at 3.7 V.

From observing the graph, it can be concluded that, in order to be able to completely charge a phone with a 800 mAh battery over the course of a day, an area of at least 270 cm^2 is required when dealing with a 3% efficiency module. If a full charge is not required, then a partial charge is possible from around 210 cm^2, providing roughly 500 mWh. Larger modules provide more power and increase the rate of charge, but there is an initial slope, from around 210 cm^2 to 300 cm^2, where a small increase in area results in a large increase in energy, which means that produced modules should be above this threshold for optimisation purposes. This region corresponds to the energy increase caused by the two effects referred

in the previous paragraph. Future progress in module efficiency will make it possible to use smaller modules, decreasing the cost and increasing convenience.

It is also important to consider the typical usage scenario for this kind of device, as it will affect the total amount of time that the module spends in the sun. In this part of the world, it is rare to find a smartphone amongst the average users, which means that the power consumption of current mobile phones is relatively low. Sources in Kampala refer brands such as Itel and Tecno as some of the main ones used throughout the country; the Itel it2020, for example, has a 1000 mAh battery and a standby time of up to 250 hours. Even if this time is not achieved, it is very common for this kind of phones to last for 2 or 3 days on a single charge. This means that 2 or 3 hours of sunlight everyday may be sufficient to keep the phone running only with solar charging, as the energy provided is enough to compensate for the energy used up since the last charge. With the increasing ubiquity of smartphones, it is expected that these devices also reach these populations sooner or later, which means that power consumption will increase.Current smartphone batteries range in capacity from 1500 mAh to more than 3000 mAh and these often need to be charged every day due to the demanding tasks performed by its users. Therefore, either larger and / or higher efficiency modules would be required for smartphone charging.

4.2 Prototype development

So as to compare and evaluate the different alternatives, four prototypes were built based on the discussion presented in the previous section:

1. Direct charger;
2. 3-battery NiMH based charger;
3. 4-battery NiMH based charger;
4. Lithium-ion polymer based charger.

4.2.1 Direct charger

From the measurements taken for figure 4.1 it was concluded that direct charging without using any electronic components should be possible, if the OPV module is produced according to certain specifications, in particular with a V_{MPP} of 5 V. The number of cells depends on the technology present on the module, but for the one used for the measurements, a 9-cell module with a Schottky diode serving both as blocking diode, to keep any external electronics from discharging through the module, and as regulated voltage drop, should work as a phone charger. In terms of current, it has a much more pronounced variation with light intensity; the

length of the module will be dependent on the amount of power needed over the course of a day. From the findings in section 4.1.3, most of the hours of sunlight during a winter day in Kampala have irradiation levels above 250 W/m^2; the J_{SC} value for this level, using the same module as before, is 2.18 mA/cm^2, which means that, in order to obtain 100 mA at 250 W/m^2, it would require a 46 cm long module. Obviously, all of this is a matter of compromise between size and available energy; for example, if the irradiation threshold is moved to 400 W/m^2, which for Kampala is from 08:00 to 16:00, the same module would only need to be 30 cm long to obtain the same current.

As previously mentioned, an alternative to precise module production control and to avoid the loss of functionality in case of degradation, a higher voltage module may be produced, in which case a voltage regulator must be used to take the higher voltage from the OPV module and output a fairly constant one at about 5 V. Keeping in mind that low cost is a priority, an LDO regulator was selected from a components catalogue which meets the following requirements:

- 6 to 8 V input voltage range;
- 5 V output voltage;
- $>$ 200 mA output current.

The NCP1117DT50G, made by ON Semiconductor, was chosen for this purpose. It has a maximum line regulation of 0.1 % and a maximum load regulation of 0.4 %. Line regulation is a measure of the ability of a circuit to maintain the output voltage with varying input voltage [16]:

$$Line\,regulation = \frac{\Delta V_o}{\Delta V_i} \tag{4.5}$$

Load regulation is a measure of the ability of a circuit to maintain the output voltage under varying load conditions [16]:

$$Load\,regulation = \frac{\Delta V_o}{\Delta I_o} \tag{4.6}$$

The maximum output current is in excess of 1.0 A and the maximum drop-out voltage is 1.2 V. In terms of power dissipation, the maximum value is given by:

$$P_D = (V_{in} - V_{out}) \times I_L + V_{in} \times I_q \tag{4.7}$$

where V_{in} is the input voltage, V_{out} is the output voltage, I_L is the load current and I_q is the quiescent current. Assuming a worst-case scenario where the input voltage is 8 V, output voltage is 4.9 V, load current is 200 mA and quiescent current is 10 mA, the total dissipated power would be 0.69 W. The data sheet of the regulator states that the thermal resistance for a DPAK case from junction

to ambient is 67°, which results in a temperature increase of about 46.2°. The efficiency of the regulator is defined as $\frac{P_{out}}{P_{in}}$; using the same values, this results in an efficiency of 58.3%. According to the regulator data sheet, two capacitors of 10 μF should be used to stabilise both the regulator itself and its output. Despite not being a problem with phones, as their internal circuits limit this effect, other electronic devices connected to the USB port may discharge through the solar module when not in use; this is an effect easily explained by looking at the equivalent circuit of a solar cell (see section 2.2). Thus, a Schottky diode with a 0.3 V forward voltage is used to prevent this from happening. An LED was added, along with a current limiting series resistor, in parallel with the USB port to indicate whether the module is working properly. The resulting circuit is represented on figure 4.5.

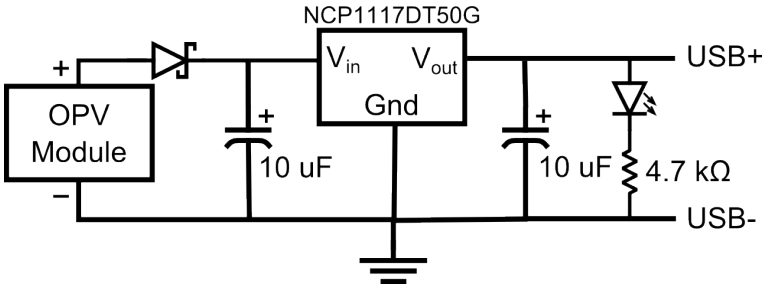

Figure 4.5: Schematic of the direct charging circuit using a voltage regulator.

The assembly of this circuit was made on a small piece of stripboard and placed inside a small plastic box, which was then stuck with double-sided adhesive tape to a strip of plastic material. This strip contains two pieces of metal tape on its inside, with small buttons at the ends, allowing an easy connection to the modules produced at Eight19, which use the same kind of buttons (figure 4.6).

Figure 4.6: Photo of the direct charging system.

As has been mentioned before, there is also the option to use a step-down converter, whose efficiency tends to be higher, although the cost also increases.

Since the objective is to quickly prototype the electronics for the charger, a pre-assembled module was purchased, the Pololu S7V8F5, which is actually both a step-down and step-up converter (buck-boost converter), with an output voltage of 5 V, input voltage range of 2.7 V to 11.8 V and maximum output current ranging from 500 mA to more than 1 A, depending on input voltage. The biggest advantage of this module is its efficiency, which at 6 V input voltage varies between 90% and 95% when the output current is less than 1.5 A.

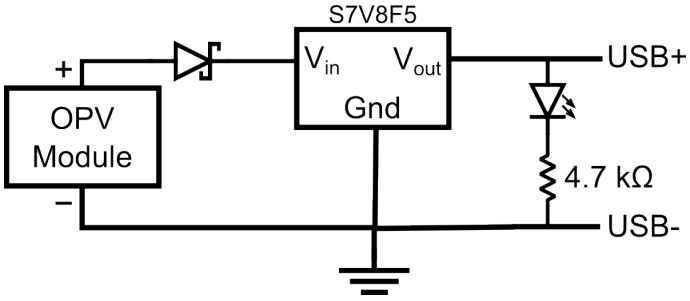

Figure 4.7: Schematic of the direct charging circuit using a buck-boost converter.

4.2.2 3-battery NiMH based charger

Using a 3-battery NiMH system, the voltage achieved from the batteries alone is around 3.6 V for most of its life cycle, though it ranges from 3 V to 4.5 V, which is not enough to charge a phone according to the USB standard. Thus, a DC-to-DC boost converter is necessary to provide 5 V. The same power module which was used on the characterisation system – the PowerPOD – was considered, but a careful look at its data sheet reveals that the maximum output current is 200 mA. Since the charging current of our model phone can go up to 800 mA, a different module was purchased (Pololu S7V8F5), which has an output current of up to 1 A when the input voltage is 3.6 V. This type of converter is known as a buck-boost converter, as it allows for voltages both lower and higher than 5 V while keeping its output constant; this feature will be useful for the 4 battery NiMH charger.

To avoid over-discharging the batteries and also to provide some information to the user of the charger, a basic battery switch and indicator were added, which cuts off power from the converter to the phone when the combined voltage drops below 3 V and lights up an LED to let the user know that it is time to charge the batteries. This was implemented using a comparator (Microchip MCP6541) to check the voltage of the batteries and a p-type MOSFET which acts as the switch when the comparator output goes to +5 V. The current draw in this "off" state is as low as possible, around 1 mA, to keep the batteries from discharging too quickly but still allow the user to get information.

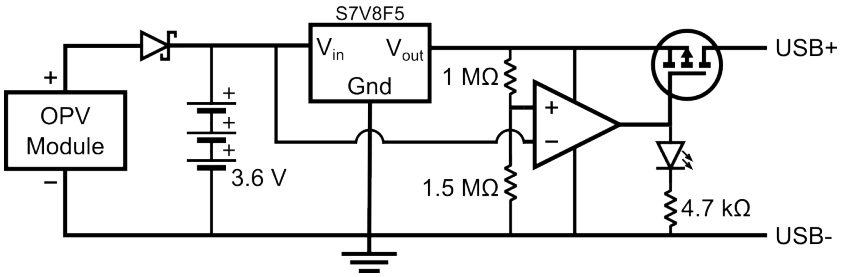

Figure 4.8: Schematic of the 3-battery NiMH charger.

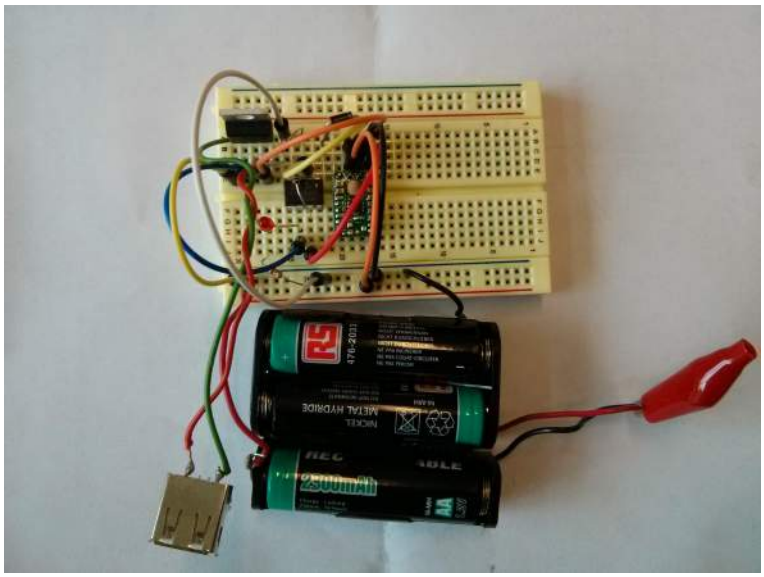

Figure 4.9: Photo of the 3-battery NiMH charging system.

4.2.3 4-battery NiMH based charger

As has been discussed above, a single NiMH battery is typically rated at 1.2 V, however there is always some variation of this value depending on the load (current flowing through the circuit) and state of charge. A fully charged NiMH battery may have a voltage at its terminals of up to 1.5 V, while if it is close to being completely discharged, the voltage could be 1 V or lower. Four of these batteries connected in series may then oscillate between 4 V and 6 V during its operation, in a worst case scenario, which is out of the voltage range required for phone charging through USB. The module used as a boost converter in the 3-battery charger is ideal for this situation, as it also works as a buck converter, effectively keeping the output voltage at 5 V, whether the input voltage is below or above this level. In this case, the input voltage range allowed by the S7V8F5 module is from 2.7 to 11.8 V.

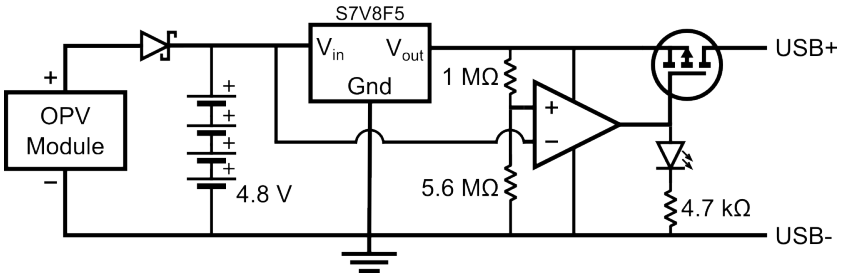

Figure 4.10: Schematic of the 4-battery NiMH charger.

Just like in the 3-battery charger, a shutdown and indicator circuit was added, with the voltage divider set to approximately 4 V instead of 3 V.

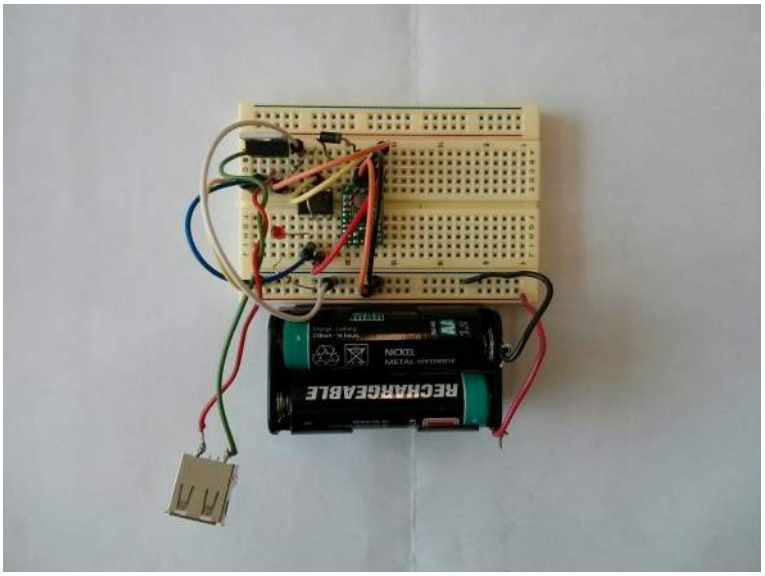

Figure 4.11: Photo of the 4-battery NiMH charging system.

4.2.4 Lithium-ion polymer based charger

In the same way as the 3-battery NiMH charger, the lithium-polymer battery charger requires a boost converter to achieve the voltage of 5 V from the lithium-polymer battery voltage of 3.7 V; the same S7V8F5 module is used here. Unlike NiMH batteries, lithium-polymer batteries are very sensitive to charging current and voltage, as can be determined from figure 4.12, which represents the charging curve of a typical lithium-polymer battery. This is known as a constant-current, constant-voltage profile, as at its initial stage, a constant current is applied to the battery to force its voltage up to a set voltage, usually 4.2 V. Once this voltage

is reached, the current is gradually decreased in order to maintain the voltage at this level.

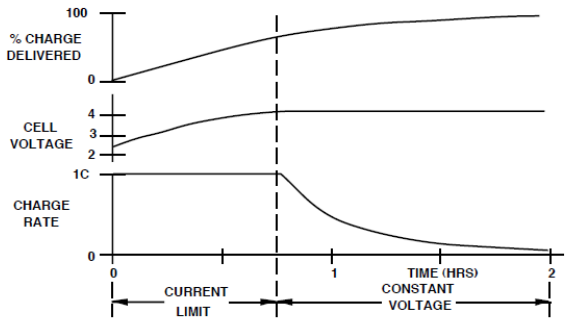

Figure 4.12: Charge profile of a lithium-polymer battery [24].

This type of charge profile must be achieved using electronics that monitor the voltage of the battery and provide current as necessary. There are ICs available specifically for this purpose, which are commonly called "battery charge controller ICs". However, these are usually SMD parts and are not practical for assembly at this stage, so an off-the-shelf module was acquired, the LiPo Charger Basic, containing an IC (Microchip MCP73831T) and the required external components.

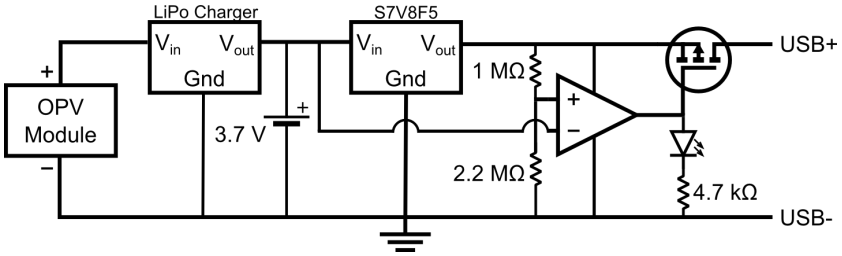

Figure 4.13: Schematic of the lithium-polymer charger.

Despite having a nominal voltage of 3.7 V, lithium-polymer batteries have a voltage range which can go from 4.2 V down to less than 3 V [6], at which point the internal circuitry inside the battery shuts down power to prevent over-discharge damage. The circuit used to inform the user and shut down the power is also used here to provide early notice of the status of the battery.

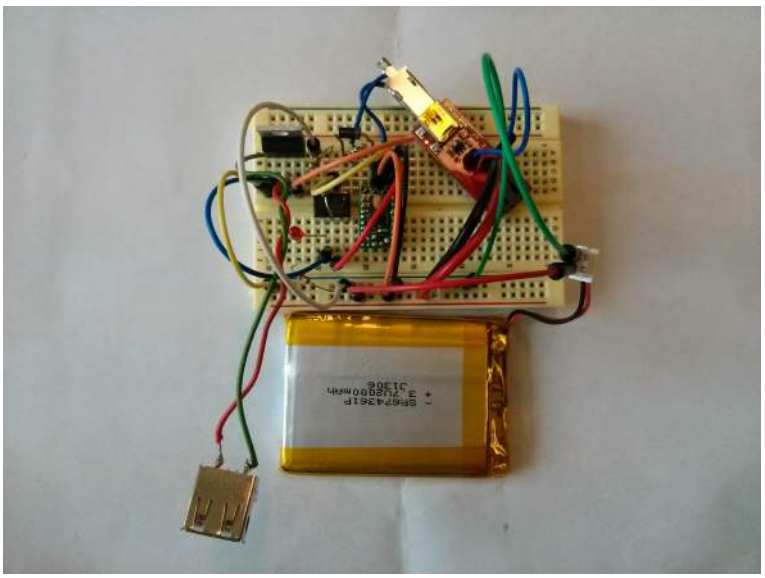

Figure 4.14: Photo of the lithium charging system.

4.3 Results and analysis

The main objective of the development of these prototypes was to gather enough information to be able to conclude mainly about the cost of the different charging options, while at the same time comparing them and recommending the best option(s). To estimate the total cost of each charger, all the components were researched on the Farnell website, using large quantity pricing to predict large-scale components cost; these values may be found on table 4.1.

Charger	Direct	Direct (with regulator)	Direct (with buck-boost)	3-battery NiMH	3-battery NiMH	Lithium-ion Polymer
Total cost	0.08£	0.59£	2.03£	5.75£	6.75£	11.79£

Table 4.1: Total cost estimate for the different chargers proposed (OPV module not included).

The production costs of the OPV module are not included as currently there is no way to accurately predict this; the same is true for other production costs such as enclosure manufacturing. As expected, the more sophisticated chargers,

with more features and useful characteristics, result in a higher production cost and therefore higher selling price. Beyond the direct versus battery issue, which was previously discussed in section 4.1.2, there is a significant difference between the direct charger using a voltage regulator and the one which uses a buck-boost converter; this difference is fundamentally due to the components required for the converter. Nonetheless, there is a key advantage that the buck-boost converter has over the voltage regulator – efficiency. This aspect is mentioned in section 4.2.1, with the efficiency value for the voltage regulator being approximately 58.3%, while the buck-boost converter is over 90 % efficient. This makes it possible to use with a smaller module, which is not only more convenient in terms of usage, but should also be slightly cheaper.

From this comparison, the direct charger which uses a buck-boost converter is recommended as being the best option for low-cost phone charging, as it offers very high efficiency, which is an essential feature when dealing with solar panels, since their intrinsic efficiency is relatively low; nevertheless, the cost of this version of the charger is low enough to be considered for the African consumer market.

Chapter 5

Conclusion and further work

The main objectives of this dissertation have been successfully achieved: a data logger to be used as an indoor light energy harvesting assessment system was developed and tested under different conditions; and four different phone charging circuit prototypes were developed, utilising different methodologies to allow for a comparison mainly focused on cost, according to the low-cost aim proposed.

The data logger uses an Arduino-like microprocessing board (Seeeduino) in conjunction with additional circuitry and is able to measure the V_{OC} and I_{SC} for a solar module, with the output being a file which is easily read by software such as Microsoft Excel. It is a portable system which can run continuously for more than 24 hours using a 2000 mAh lithium-ion polymer battery. Several test measurements were made and are presented in the main chapter concerning this topic. These measurements reflect the dependence of solar module performance with the weather and provide values such as the total energy possible to collect during a day, therefore providing information which can be easily used to predict application viability and suitability.

Regarding phone charging, the different prototypes were successfully developed and, in conjunction with the research done for usage scenarios and available energy, provide valuable information for a low-cost phone charging application in Africa. The cost analysis presented at the end of chapter 4, along with the discussion, allows for a comparison between the different versions and the advantages and drawbacks of each one. The recommendation given is that the most appropriate charger for the intended purpose is the direct charger with a buck-boost converter.

Concerning all the prototypes developed during the duration of the internship, there is some room for improvement in certain aspects, which shall be here discussed. The data logger, while originally planned for accepting different kinds of modules, currently only works with small modules, with around 27 cm^2 of area. To enable the use of larger modules would require a way to measure a wider range of voltage and current, which means that the gain of the amplifiers would have to be changed. This could be done either by setting a different fixed gain or by

adding potentiometers to control the two gains. A further improvement which would bring significant advances would be the possibility to trace a complete I-V curve for the module, which could be implemented by connecting a DAC to the Seeeduino to provide different voltages to the module, while measuring current at the same time. One more modification which might be useful to add would be light, temperature and humidity sensors in order to better relate module performance with these characteristics from he environment. For the phone charging systems, the next step to test would be the use of a custom made module with a V_{MPP} of about 5 V at 1 sun and sufficient current to exceed the 100 mA threshold for phone charging. This would equate to the lowest cost charger possible, which was one of the initial purposes of this thesis.

Bibliography

[1] Advanced Linear Devices. Performance characteristics of EPAD precision matched pair MOSFET family. 2012.

[2] Ahmad, J., Bazaka, K., Anderson, L. J., White, R. D., and Jacob, M. V. Materials and methods for encapsulation of OPV: A review. *Renewable and Sustainable Energy Reviews 27* (Nov. 2013), 104–117.

[3] Arduino. Arduino - Introduction. Available at `http://www.arduino.cc/en/Guide/Introduction`, accessed on 15/6/2014.

[4] Brabec, C. J., Gowrisanker, S., Halls, J. J. M., Laird, D., Jia, S., and Williams, S. P. Polymer-fullerene bulk-heterojunction solar cells. *Advanced materials (Deerfield Beach, Fla.) 22*, 34 (Sept. 2010), 3839–56.

[5] Brown Dog Solar. Kick Back 3W USB Solar Cell. Available at `http://browndogsolar.com/collections/solar-cells/products/kick-back-3-6w-solar-cell`, accessed on 27/6/2014.

[6] Buchmann, I. Will Lithium-Ion batteries power the new millennium ? Tech. rep., Cadex Electronics Inc., 2001.

[7] Cook, E. *Man, Energy and Society.* W. H. Freeman, 1976.

[8] EnOcean GmbH. EnOcean Technology – Energy Harvesting Wireless. 2011.

[9] ESMAP, and The World Bank. Power Sector Reform in Africa: Assessing Impact on Poor People. Tech. rep., 2005.

[10] European Comission. JRC's Institute for Energy and Transport - PVGIS. Available at `http://re.jrc.ec.europa.eu/pvgis/`, accessed on 17/6/2014.

[11] Hernday, P. Field Applications for I-V Curve Tracers. *SolarPro*, 4.5 (2011).

[12] Hersch, P., and Zweibel, K. *Basic photovoltaic principles and methods.* Technical Information Office, Solar Energy Research Institute, 1982.

[13] Intel, Compaq, Hewlett-packard, Microsoft, Lucent, Philips, and NEC. Universal Serial Bus 2.0 Specification. Tech. rep., 2000.

[14] Intel, Hewlett-packard, Microsoft, ST-Ericsson, NEC, and Instruments, T. Universal Serial Bus 3.0 Specification. Tech. rep., 2011.

[15] Jø rgensen, M., Norrman, K., and Krebs, F. C. Stability/degradation of polymer solar cells. *Solar Energy Materials and Solar Cells 92*, 7 (July 2008), 686–714.

[16] Lee, B. S. Understanding the Terms and Definitions of LDO Voltage Regulators. Tech. Rep. October, 1999.

[17] Li, G., Zhu, R., and Yang, Y. Polymer solar cells. *Nature Photonics 6*, 3 (Feb. 2012), 153–161.

[18] Lorenzo, E. *Solar Electricity: Engineering of Photovoltaic Systems*. 1994.

[19] Luque, A., and Hegedus, S. *Handbook of Photovoltaic Science and Engineering*. Wiley, 2003.

[20] National Instruments. How to Minimize Errors for Low-Current Measurements. 2–4.

[21] Seeed Studio. Seeeduino v3.0. Available at `http://www.seeedstudio.com/wiki/Seeeduino_v3.0`, accessed on 18/4/2014.

[22] Shaheen, S. E., Ginley, D. S., and Jabbour, G. E. Organic-Based Photovoltaics : Toward Low-Cost Power Generation. *MRS Bulletin 30*, January (2005), 10–19.

[23] Sharpe, L. T., Stockman, A., Jagla, W., and Jägle, H. A luminous efficiency function, V*(lambda), for daylight adaptation. *Journal of vision 5*, 11 (Jan. 2005), 948–68.

[24] Simpson, C. Battery Charging. Tech. rep., Texas Instruments, 2011.

[25] Steim, R., Ameri, T., Schilinsky, P., Waldauf, C., Dennler, G., Scharber, M., and Brabec, C. J. Organic photovoltaics for low light applications. *Solar Energy Materials and Solar Cells 95*, 12 (Dec. 2011), 3256–3261.

[26] Su, Y.-W., Lan, S.-C., and Wei, K.-H. Organic photovoltaics. *Materials Today 15*, 12 (Dec. 2012), 554–562.

Appendices

Appendix A

List of components: data logger

The following is a list of components used in the development of the module characterisation system (see figure 3.4 for schematic).

Manufacturer	Component	Description
Seeed Studio	Seeeduino V3.0	Arduino-like microcontroller prototyping board
Ciseco	I/O POD RTC	Real-time clock module based on the BQ32000 IC by Texas Instruments
Ciseco	I/O POD microSD Card	μSD card socket module
Ciseco	PowerPOD NCP1402 5V0	5V power supply module based on the NCP1402 IC by ON Semiconductor
Microchip	MCP6291	Single-supply operational amplifier, 1 mA, 10 MHz
Fairchild Semiconductor	2N7000	N-Channel enhancement mode MOSFET, 60 V, 0.2 A
RS	DIP05-1A72-BV710	Reed relay, SPST-NO, 1A, 5V DC

Appendix B

List of components: phone chargers

The following is a list of components used in the development of the different phone charging prototypes, as seen on section 4.2.

B.1 Direct chargers

Manufacturer	Component	Description
ON Semiconductor	1N5817RLG	Schottky rectifier diode, 1 A, 20 V
ON Semiconductor	NCP1117DT50G	Low-dropout voltage regulator, 1 A, 5 V
Kemet	T356E106K025AT	10 ± 10% μF 25 V tantalum capacitor
Nichia	NSPW315DS	3 mm White LED, 70°, 1840-5040 mcd
Pololu	S7V8F5	5 V step-up step-down DC-to-DC converter

B.2 NiMH based chargers

Manufacturer	Component	Description
ON Semiconductor	1N5817RLG	Schottky rectifier diode, 1 A, 20 V
Pololu	S7V8F5	5 V step-up step-down DC-to-DC converter
RS	476-2033	1.2 V NiMH AA rechargeable battery, 2300 mAh
Microchip	MCP6541-E/P	Comparator, single-supply, push-pull
ON Semiconductor	NTP2955G	P-channel MOSFET, 60 V, 12 A
Kingbright	L-7104SRD-J4	3 mm Red LED, 40°, 1.5 cd

B.3 Lithium-ion polymer based charger

Manufacturer	Component	Description
Sparkfun	PRT-10401	LiPo charger module based on the MCP73831T IC by Microchip
MikroElektronika	MIKROE-1120	3.7 V lithium-ion polymer battery, 2000 mAh
Pololu	S7V8F5	5 V step-up step-down DC-to-DC converter
Microchip	MCP6541-E/P	Comparator, single-supply, push-pull
ON Semiconductor	NTP2955G	P-channel MOSFET, 60 V, 12 A
Kingbright	L-7104SRD-J4	£ mm Red LED, 40°, 1.5 cd

Appendix C

Seeeduino code

```
#include <SD.h>
#include <Wire.h>
#include "RTClib.h"
#include <JeeLib.h>

File logfile;
RTC_DS1307 rtc;
ISR(WDT_vect) {
  Sleepy::watchdogEvent();
}

double voltage[20];
double current[20];
double volt_avg, curr_avg;
double t;

void setup(){

  pinMode(5, OUTPUT);
  digitalWrite(5, HIGH);

  Serial.begin(9600);
#ifdef AVR
  Wire.begin();
#else
  Wire1.begin(); // Shield I2C pins connect to alt I2C bus
      on Arduino Due
#endif
  rtc.begin();
```

```
  //rtc.adjust(DateTime(__DATE__, __TIME__)); //only
     needed once (must be connected to comp)
  DateTime now = rtc.now();

  pinMode(4, OUTPUT);
  if (!SD.begin(4)) {
    delay(100);
    digitalWrite(5, LOW);
    delay(100);
    return;
  }

  logfile = SD.open("log.txt", FILE_WRITE);
  if (logfile) {
    logfile.print("# Hello! The date is ");
    logfile.print(now.day(), DEC);
    logfile.print('/');
    logfile.print(now.month(), DEC);
    logfile.print('/');
    logfile.print(now.year(), DEC);
    logfile.println('.');
    logfile.print("Timestamp");
    logfile.print("\t");
    logfile.print("Time");
    logfile.print("\t");
    logfile.print("Voltage (mV)");
    logfile.print("\t");
    logfile.println("Current (uA)");
  }
  logfile.close();

  pinMode(7, INPUT);
  pinMode(2, OUTPUT);
  digitalWrite(2, LOW);
  delay(10);
  t = 0;

}

void loop(){
  if (!SD.begin(4)) {
    // Reset if there is no SD card
```

```
  setup();
}

DateTime now = rtc.now();

volt_avg = 0;
curr_avg = 0;

// Slow mode - one set of measurements every 5 minutes
if (digitalRead(7) == HIGH){

  for (int i=0; i<40; i++){
    int vread = analogRead(0);
    volt_avg = volt_avg + (vread * 3.3 / 1024.0);
    analogWrite(5, 255 - i * 5);
    delay(10);
  }
  volt_avg = volt_avg / 40.0 * 1000; // average and
     convert to millivolt
  volt_avg = ((volt_avg + 2.643) / 0.6511); //
     calibration

  digitalWrite(2, HIGH);
  delay(50);

  for (int i=0; i<40; i++){
    int iread = analogRead(1);
    curr_avg = curr_avg + (iread * 3.3 / 1024.0);
    analogWrite(5, 55 + i * 5);
    delay(10);
  }
  curr_avg = curr_avg / 40.0 * 1000; // average and
     convert to millivolt
  curr_avg = ((curr_avg - 0.302) / 0.3277); //
     calibration

  t = t + 300;

  logfile = SD.open("log.txt", FILE_WRITE);
  logfile.print(now.hour(), DEC);
  logfile.print(':');
  logfile.print(now.minute(), DEC);
```

```
    logfile.print(':');
    logfile.print(now.second(), DEC);
    logfile.print("\t");
    logfile.print(t);
    logfile.print("\t");
    logfile.print(volt_avg, 3);
    logfile.print("\t");
    logfile.println(curr_avg, 3);
    logfile.close();

    digitalWrite(2, LOW);
    delay(50);

    // Sleep for about 5 minutes to save power - only
       saves a few milliamps,
    // not suitable for long term (probably due to voltage
        regulator)
    for (byte i = 0; i < 5; ++i)
      Sleepy::loseSomeTime(60000);
  }

  // Fast mode - one set of measurements every half second
  if (digitalRead(7) == LOW){

    for (int i=0; i<20; i++){
      int vread = analogRead(0);
      volt_avg = volt_avg + (vread * 3.3 / 1024.0);
      analogWrite(5, 255 - i * 10);
      delay(10);
    }
    volt_avg = volt_avg / 20.0 * 1000; // average and
       convert to millivolt
    volt_avg = ((volt_avg + 2.643) / 0.6511); //
       calibration

    digitalWrite(2, HIGH);
    delay(50);

    for (int i=0; i<20; i++){
      int iread = analogRead(1);
      curr_avg = curr_avg + (iread * 3.3 / 1024.0);
      analogWrite(5, 55 + i * 10);
```

```
      delay(10);
    }
    curr_avg = curr_avg / 20.0 * 1000; // average and
       convert to millivolt
    curr_avg = ((curr_avg - 0.302) / 0.3277); //
       calibration

    t = t + .5;

    logfile = SD.open("log.txt", FILE_WRITE);
    logfile.print(now.hour(), DEC);
    logfile.print(':');
    logfile.print(now.minute(), DEC);
    logfile.print(':');
    logfile.print(now.second(), DEC);
    logfile.print("\t");
    logfile.print(t);
    logfile.print("\t");
    logfile.print(volt_avg, 3);
    logfile.print("\t");
    logfile.println(curr_avg, 3);
    logfile.close();

    digitalWrite(2, LOW);
    delay(50);
  }
}
```